RESEARCH MEMORANDUM

for the

Air Materiel Command, Army Air Forces

ALTITUDE-WIND-TUNNEL INVESTIGATION OF PERFORMANCE OF SEVERAL PROPELLERS ON YP-47M AIRPLANE AT HIGH BLADE LOADINGS

V - CURTISS 836-14C2-18R1 FOUR-BLADE PROPELLER

By Martin J. Saari and Lewis E. Wallner

Aircraft Engine Research Laboratory
Cleveland, Ohio

NATIONAL ADVISORY COMMITTEE FOR AERONAUTICS

WASHINGTON

Dec. 2, 1946

NATIONAL ADVISORY COMMITTEE FOR AERONAUTICS

RESEARCH MEMORANDUM

for the

Air Materiel Command, Army Air Forces

ALTITUDE-WIND-TUNNEL INVESTIGATION OF PERFORMANCE OF SEVERAL PROPELLERS ON YP-47M AIRPLANE AT HIGH BLADE LOADINGS

V - CURTISS 836-14C2-18R1 FOUR-BLADE PROPELLER

By Martin J. Saari and Lewis E. Wallner

SUMMARY

An altitude-wind-tunnel investigation has been made to determine the performance of a Curtiss 836-14C2-18R1 four-blade propeller on a YP-47M airplane at high blade loadings and high engine powers. The study was made for a range of power coefficients from 0.10 to 1.00 at free-stream Mach numbers of 0.30, 0.40, and 0.50. The results of the force measurements indicate primarily the trend of propeller efficiency for changes in power coefficient or advance-diameter ratio, inasmuch as no corrections for the effects of tunnel-wall constriction on the installation were applied. Slipstream surveys are presented to illustrate blade thrust load distribution for several operating conditions.

For the range of advance-diameter ratios investigated at a free-stream Mach number of 0.30, highest efficiencies were obtained at power coefficients from 0.10 to 0.30 and flow breakdown was evident for power coefficients above 0.40.

The maximum efficiencies at a free-stream Mach number of 0.40 were obtained for power coefficients from 0.20 to 0.40, between advance-diameter ratios of 1.50 and 3.10. The envelope of the efficiency curves decreased about 15 percent between advance-diameter ratios of 2.20 and 3.80.

At a free-stream Mach number of 0.50, maximum efficiency in the low range of advance-diameter ratios was obtained for a power

coefficient of 0.30, and in the high range of advance-diameter ratios at a power coefficient of 1.00. There was about a 4 percent decrease in the envelope of the efficiency curves between advance-diameter ratios of 2.20 and 3.60.

INTRODUCTION

An investigation of the performance of several propellers on the YP-47M airplane at high blade loadings has been conducted in the Cleveland altitude wind tunnel at the request of the Air Materiel Command, Army Air Forces. As part of the program, a study was made of a Curtiss 836-14C2-18R1 four-blade propeller.

The investigation was made for a range of power coefficients from 0.10 to 1.00 at free-stream Mach numbers of 0.30, 0.40, and 0.50 for density altitudes from 10,000 to 45,000 feet, engine powers from 150 to 2500 brake horsepower, and for engine speeds from 1000 to 2900 rpm.

The propeller efficiencies were obtained from force measurements and the blade thrust load distribution was obtained by two diametrically opposed slipstream survey rakes as in references 1 to 4.

PROPELLER AND POWER PLANT

A description of the propeller and the power plant is as follows:

Propeller	
Blade design	Curtiss 836-14C2-18R1
Number of blades	four
Blade sections	NACA 16 series
Propeller diameter	13 feet, 0 inch
Activity factor[1]	98
Propeller gear ratio	20:9
Engine	R-2800-73
War emergency power rating:	
Engine speed, rpm	2800
Manifold pressure, in. Hg	72.0
Brake horsepower	2800
Military power rating:	
Engine speed, rpm	2800
Manifold pressure, in. Hg	53.5
Brake horsepower	2100

Normal power rating:	
Engine speed, rpm	2600
Manifold pressure, in. Hg	41.5
Brake horsepower	1700

[1]The activity factor is a nondimensional function of the propeller plan form designed to express the integrated capacity of the propeller blade elements for absorbing power (reference 1).

The propeller blade-form characteristics are given in figure 1. A photograph of a Curtiss 836-14C2-18R1 propeller blade is shown in figure 2.

APPARATUS AND METHODS

The assembled propeller as installed on the YP-47M airplane in the 20-foot-diameter test section of the altitude wind tunnel is shown in figure 3. A description of the other equipment is given in reference 1.

The investigation was made for a range of power coefficients from 0.10 to 1.00 at free-stream Mach numbers of 0.30, 0.40, and 0.50. Density altitudes from 10,000 to 45,000 feet were simulated for a range of engine powers from 150 to 2500 brake horsepower and engine speeds from 1000 to 2900 rpm.

REDUCTION OF DATA

The method of data reduction was the same as that described in reference 1. The force measurements were analyzed in terms of the variation of the propeller efficiency η with the propeller power coefficient C_P and the advance-diameter ratio J. These quantities were computed from the following equations:

$$C_P = \frac{P}{\rho n^3 D^5}$$

where

D propeller diameter, feet

n propeller rotational speed, revolutions per second

P engine power, foot-pounds per second

ρ free-stream density, slugs per cubic foot

$$J = \frac{V}{nD}$$

where

V free-stream velocity, feet per second

$$\eta = \frac{C_T J}{C_P}$$

The propeller thrust coefficient C_T in the efficiency formula was defined as

$$C_T = \frac{T}{\rho n^2 D^4}$$

where

T propeller thrust, pounds

Propeller tip Mach number M_t was obtained from the equation

$$M_t = M_O \sqrt{1 + \left(\frac{\pi}{J}\right)^2}$$

where

M_O free-stream Mach number

The slipstream surveys were presented as plots of the total-pressure differential $H_s - H_O$ against the square of the radius ratio $(r_s/R)^2$ where

H_O free-stream total pressure, pounds per square foot

H_s total pressure at survey point, pounds per square foot

R propeller radius to tip, inches

r_s radial distance from thrust axis to survey point, inches

RESULTS AND DISCUSSION

The results of the force measurements are primarily of value in showing the trend of propeller efficiency for changes in power coefficient or advance-diameter ratio. The absolute efficiency values are questionable because an average drag coefficient for the installation was used for all the propellers investigated. Data obtained at different free-stream Mach numbers are not comparable because corrections for tunnel-wall constriction effects, which vary with airspeed, have not been applied. (See reference 1.) Slipstream surveys are presented to illustrate the blade thrust load distribution for several operating conditions.

Free-stream Mach number, 0.30. - The effect of advance-diameter ratio on the propeller efficiency at a free-stream Mach number of 0.30 is shown in figure 4 for a range of power coefficients from 0.10 to 1.00. The variation of propeller efficiency with power coefficient is shown in figure 5 for approximately constant values of advance-diameter ratio. For the range of advance-diameter ratios investigated, highest efficiencies were obtained at power coefficients from 0.10 to 0.30. In general, large reductions in efficiency due to flow breakdown were evident at power coefficients above 0.40. (See figs. 4 and 5.)

The effect of power coefficient on the blade thrust load distribution is shown by the slipstream surveys in figure 6, which correspond to the conditions of figure 5 for $J \approx 1.00$. The blade thrust loading was relatively low and uniformly distributed over the blade span for a power coefficient of 0.10. (See fig. 6(a).) An increase in power coefficient from 0.10 to 0.30 increased the thrust loading considerably and the maximum thrust was obtained at $(r_s/R)^2 = 0.65$, or at about 80 percent of the blade span. (See figs. 6(b) and 6(c).) The over-all thrust loading increased with a change in power coefficient from 0.30 to 0.40. The maximum load however, shifted inboard to $(r_s/R)^2 = 0.50$, indicating that flow breakdown occurred on the tip sections. (See fig. 6(d).) This flow breakdown, which could be attributed to a combination of stall and compressibility effects, became more prominent as the power coefficient was increased from 0.40 to 0.68. (See figs. 6(e) to 6(g).)

The difference between the right and the left surveys was apparently due to a slight inclination of the approaching air stream to the thrust axis. (See reference 5.)

The effect of advance-diameter ratio on the blade thrust load distribution is shown by slipstream surveys in figures 7 and 8, which correspond to the conditions of figure 4, for power coefficients of 0.20 and 0.40, respectively. At a power coefficient of 0.20, a reduction in advance-diameter ratio from 2.00 to 1.32 (figs. 7(a) to 7(c)) increased the over-all thrust loading considerably. When the advance-diameter ratio was decreased from 1.32 to 1.00 (figs. 7(c) and 7(d)) there was a reduction in over-all thrust; however, this reduction in thrust loading was due to the higher altitude and lower engine power at which the advance-diameter ratio of 1.00 was obtained. At a power coefficient of 0.40 (fig. 8), a change in advance-diameter ratio from 2.04 to 1.16 resulted in a more rapid increase of thrust loading on the outboard sections than on the inboard sections. A further change in advance-diameter ratio from 1.16 to 1.01 increased the over-all thrust loading, and flow breakdown became evident on sections outboard of $(r_s/R)^2 \approx 0.55$.

Free-stream Mach number, 0.40. - The effect of advance-diameter ratio on the propeller efficiency at a free-stream Mach number of 0.40 is shown in figure 9 for a range of power coefficients from 0.10 to 1.00. The variation of propeller efficiency with power coefficient is shown in figure 10 for approximately constant values of advance-diameter ratio.

Highest efficiencies were obtained at power coefficients from 0.20 to 0.40 at advance-diameter ratios from 1.50 to 3.10. The envelope of the efficiency curves decreased about 15 percent between advance-diameter ratios of 2.20 and 3.80. (See fig. 9.) As the power coefficient was increased, the peak efficiency occurred at generally increasing values of advance-diameter ratio. In the low range of advance-diameter ratios large reductions in efficiency due to blade stall were evident at the high power coefficients. For example, at an advance-diameter ratio of 1.70, a change in power coefficient from 0.60 to 0.70 resulted in a 24-percent reduction in propeller efficiency.

The effect of power coefficient on blade thrust load distribution is shown by the slipstream surveys in figure 11, which correspond to conditions of figure 10 for $J \approx 1.70$. The blade thrust load distributions were similar for power coefficients from 0.10 to 0.60, and the maximum loading occurred on sections at about $(r_s/R)^2 = 0.70$. (See figs. 11(a) to 11(e).) Blade stall was evident at power coefficients of 0.71 and 0.92. (See figs. 11(f) and 11(g).) The magnitudes of the thrust loadings shown in figure 11 cannot be compared, inasmuch as the surveys were obtained at different density altitudes.

Blade thrust load distribution curves, which correspond to the conditions of figure 9 for power coefficients of 0.30 and 0.70, are presented in figures 12 and 13, respectively. At a power coefficient of 0.30 and an advance-diameter ratio of 3.00, the thrust loading was uniformly distributed over the blade span. (See fig. 12(a).) As the advance-diameter ratio was decreased from 2.36 to 1.67 (figs. 12(b) and 12(c)), the thrust loading increased more rapidly on the tip sections than on the inboard sections. Compressibility losses became evident on sections outboard of $(r_s/R)^2 = 0.65$ at an advance-diameter ratio of 1.38, which corresponds to a tip Mach number of 0.98. (See fig. 12(d).) At a power coefficient of 0.71 and an advance-diameter ratio of 3.85 (fig. 13(a)), the thrust loading was slightly greater on the inboard sections than on the tip sections. However, as the advance-diameter ratio was reduced from 3.85 to 2.09 the thrust loading on the tip sections increased more rapidly than on the inboard sections. (See figs. 13(a) to 13(c).) When the advance-diameter ratio was further reduced to 1.66 and 1.50, blade stall became evident on sections outboard of $(r_s/R)^2 = 0.45$, and the loading on the inboard sections increased. (See figs. 13(d) and 13(e).) The angle of attack at which the stall occurred was probably reduced by the high operating tip Mach number. (See reference 6.)

Free-stream Mach number, 0.50. - The effect of advance-diameter ratio on the propeller efficiency at a free-stream Mach number of 0.50 is shown in figure 14 for power coefficients from 0.10 to 1.00. The variation of propeller efficiency with power coefficient is shown in figure 15 for approximately constant values of advance-diameter ratio.

Maximum efficiency in the low range of advance-diameter ratio was obtained for a power coefficient of 0.30, and in the high range of advance-diameter ratio for a power coefficient of 1.00. Between advance-diameter ratios of 2.20 and 3.60, there was a decrease of about 4 percent in the envelope of the efficiency curves. (See fig. 14.) The advance-diameter ratio for peak efficiency increased generally as the power coefficient was increased (fig. 14).

The effect of power coefficient on blade thrust load distribution is shown in figures 16 and 17, which correspond to the conditions of figure 15 for advance-diameter ratios of approximately 2.20 and 4.30, respectively. At an advance-diameter ratio of 2.20, the thrust loading was slightly greater on the tip sections than on the inboard sections, and the loading increased

uniformly over the blade as the power coefficient was increased from 0.10 to 0.41. (See figs. 16(a) to 16(d).) At a power coefficient of 0.60 a slight reduction in thrust loading, resulting from compressibility effects, occurred at sections beyond $(r_s/R)^2 = 0.60$. (See fig. 16(e).) The blade thrust loading for an advance-diameter ratio of approximately 4.30 was uniform and similar for power coefficients from 0.51 to 1.03. (See fig. 17.)

Slipstream surveys for a range of advance-diameter ratios are shown in figures 18, 19, and 20 for power coefficients of approximately 0.20, 0.60, and 1.00, respectively. At a power coefficient of 0.21 and an advance-diameter ratio of 3.45 (fig. 18(a)), the thrust loading on the inboard sections was slightly higher than on the tip sections. However, as the advance-diameter ratio was reduced to 2.26 (figs. 18(b) and 18(c)), the loading on the tip sections increased more rapidly than on the inboard sections. At an advance-diameter ratio of 1.78, which corresponds to a tip Mach number of 1.02, compressibility losses were evident on sections outboard of $(r_s/R)^2 = 0.50$. (See fig. 18(d).) At a power coefficient of 0.60, a change in advance-diameter ratio from 4.30 to 2.25 (figs. 19(a) to 19(e)) resulted in a shift of the maximum thrust loading from the inboard sections to the tip sections. Compressibility effects were evident on sections beyond $(r_s/R)^2 = 0.70$ at an advance-diameter ratio of 2.16 and a tip Mach number of 0.89 (fig. 19(f)). A further decrease in advance-diameter ratio to 1.70, which corresponds to a tip Mach number of 1.01, resulted in compressibility effects as far inboard as $(r_s/R)^2 = 0.50$. The blade thrust loading increased, but the load distribution remained uniform for the range of advance-diameter ratios investigated at a power coefficient of 1.00. (See fig. 20.)

SUMMARY OF RESULTS

Because corrections for tunnel-wall constriction have not been applied, the propeller efficiencies presented in this report are useful primarily in showing the comparative effects of blade loading on propeller performance. The investigation in the altitude wind tunnel of the performance at high blade loadings of a Curtiss 836-14C2-18R1 four-blade propeller on a YP-47M airplane indicated that:

1. For the range of advance-diameter ratios investigated at a free-stream Mach number of 0.30, highest efficiencies were obtained at power coefficients from 0.10 to 0.30 and flow breakdown was evident for power coefficients above 0.40.

2. Highest efficiencies at a free-stream Mach number of 0.40 were obtained for power coefficients from 0.20 to 0.40 at advance-diameter ratios from 1.50 to 3.10. The envelope of efficiency curves decreased about 15 percent between advance-diameter ratios of 2.20 and 3.80.

3. At a free-stream Mach number of 0.50, maximum efficiency in the low range of advance-diameter ratios was obtained for a power coefficient of 0.30, and in the high range of advance-diameter ratios at a power coefficient of 1.00. The envelope of the efficiency curves decreased about 4 percent between advance-diameter ratios of 2.20 and 3.60.

4. In general, below the stall the local thrust loading was a maximum on the tip sections at the low advance-diameter ratios and a maximum on the inboard sections at the high advance-diameter ratios. As stall developed at the blade tips the maximum thrust loading shifted toward the inboard sections of the blades.

Aircraft Engine Research Laboratory,
National Advisory Committee for Aeronautics,
Cleveland, Ohio.

Martin J. Saari,
Aeronautical Engineer.

Lewis E. Wallner,
Mechanical Engineer.

Approved:

Alfred W. Young,
Mechanical Engineer.

Abe Silverstein,
Aeronautical Engineer.

rl

REFERENCES

1. Saari, Martin J., and Wallner, Lewis E.: Altitude-Wind-Tunnel Investigation of Performance of Several Propellers on YP-47M Airplane at High Blade Loading. I - Aeroproducts H2OC-162-X11M2 Four-Blade Propeller. NACA RM No. E6I24, Army Air Forces, 1946.

2. Wallner, Lewis, E., and Sorin, Solomon M.: Altitude-Wind-Tunnel Investigation of the Performance of Several Propellers on YP-47M Airplane at High Blade Loading. II - Curtiss 838-1C2-18R1 Four-Blade Propeller. NACA RM No. E6J14, Army Air Forces, 1946.

3. Saari, Martin J., and Converse, Arthur N.: Altitude-Wind-Tunnel Investigation of Performance of Several Propellers on YP-47M Airplane at High Blade Loadings. III - Hamilton Standard A6543A-0 Four-Blade Propeller. NACA RM No. E6J22, Army Air Forces, 1946.

4. Saari, Martin J., and Sorin, Solomon M.: Altitude-Wind-Tunnel Investigation of Performance of Several Propellers on YP-47M Airplane at High Blade Loadings. IV - Curtiss 732-1C2-0 Four-Blade Propeller. NACA RM No. E6J23, Army Air Forces, 1946.

5. Pendley, Robert E.: Effect of Propeller-Axis Angle of Attack on Thrust Distribution over the Propeller Disk in Relation to Wake-Survey Measurement of Thrust. NACA ARR No. L5J02b, 1945.

6. Sprieter, John R., and Steffen, Paul J.: Effect of Mach and Reynolds Numbers on Maximum Lift Coefficient. NACA TN No. 1044, 1946.

INDEX OF FIGURES

Page

Page

Page

Page

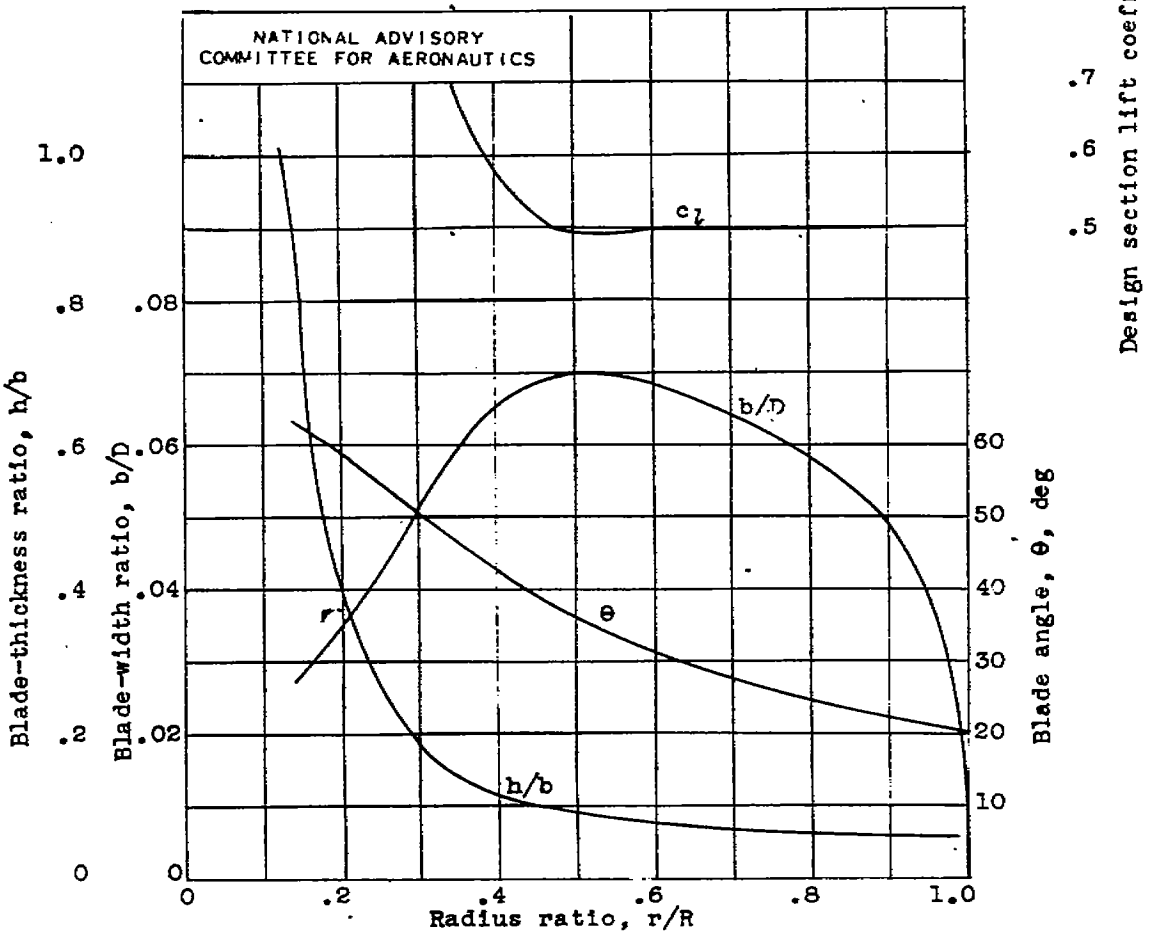

Figure 1.- Blade-form curves for Curtiss 836-14C2-18R1 four-blade propeller. b, section chord; D, diameter; h, section thickness; R, radius to tip; r, section radius.

836-14C2-18R1

NACA
C-13547
10-26-45

Figure 2. - Curtiss 836-14C2-18R1 propeller blade.

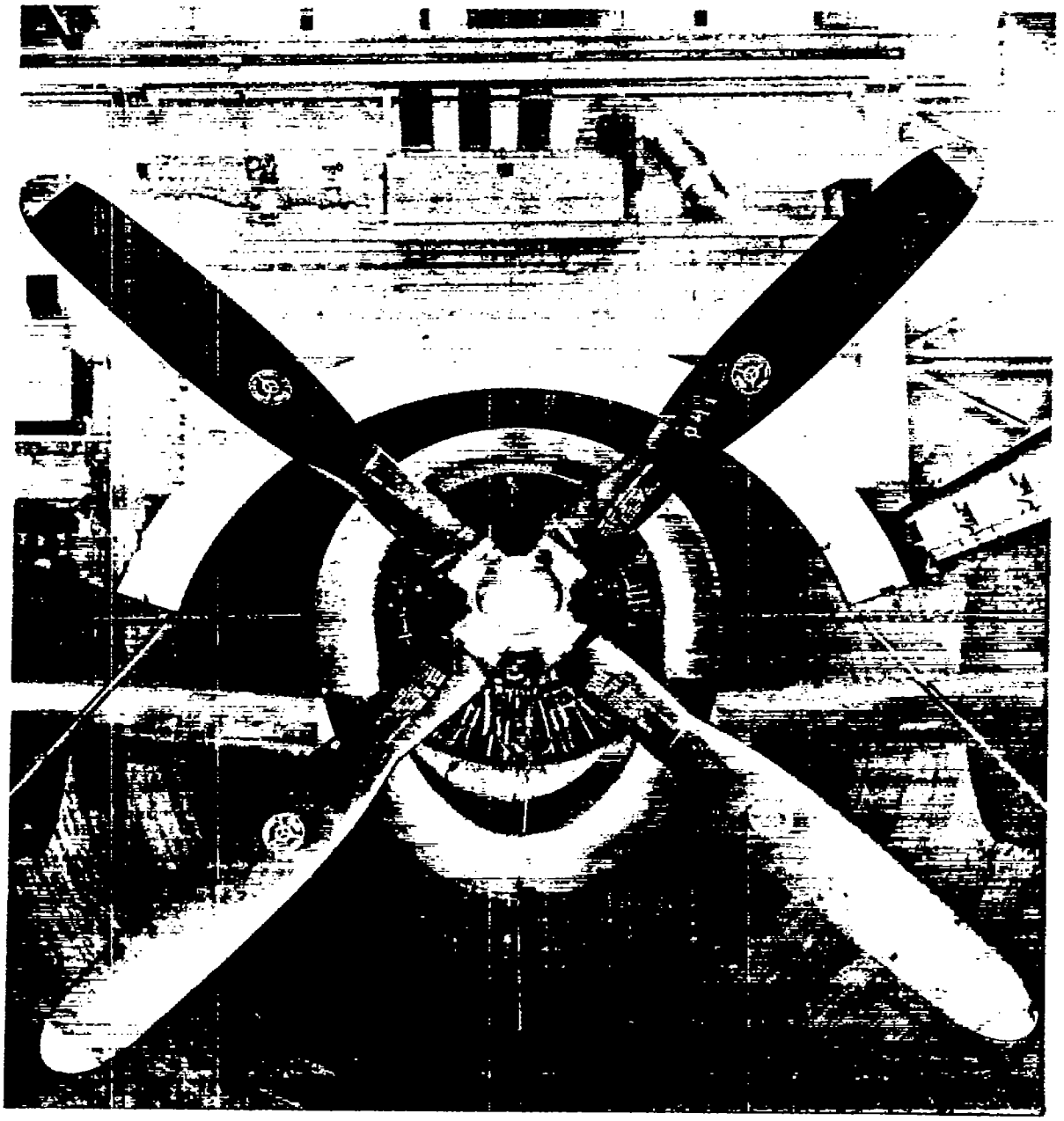

NACA
C-13482
9-27-45

Figure 3. - Front view of YP-47M airplane with Curtiss 836-14C2-18R1 four-blade propeller installed in altitude-wind-tunnel test section.

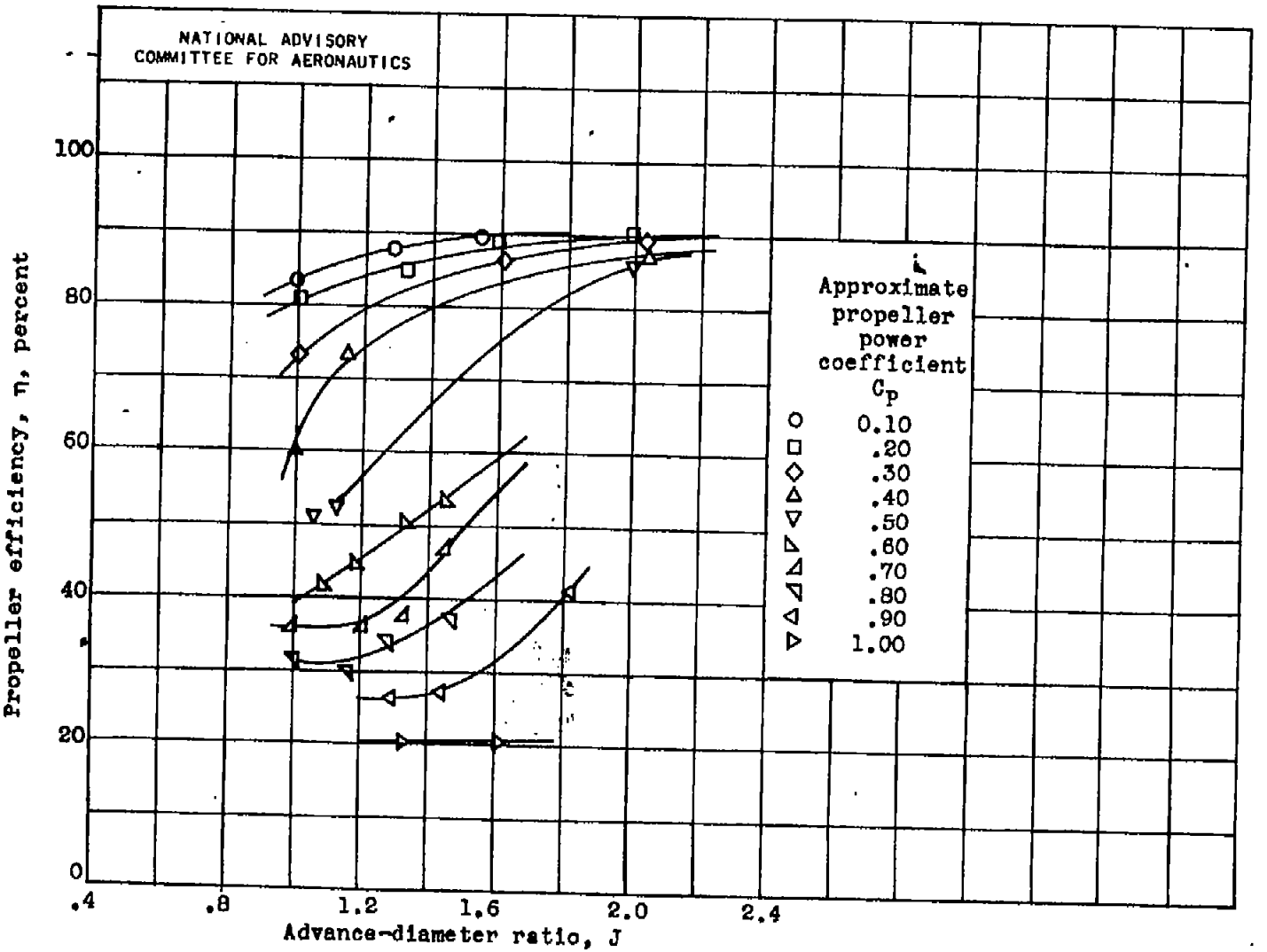

Figure 4.- Characteristics of Curtiss 836-14C2-18R1 four-blade propeller on YP-47M airplane at free-stream Mach number M_o of approximately 0.30.

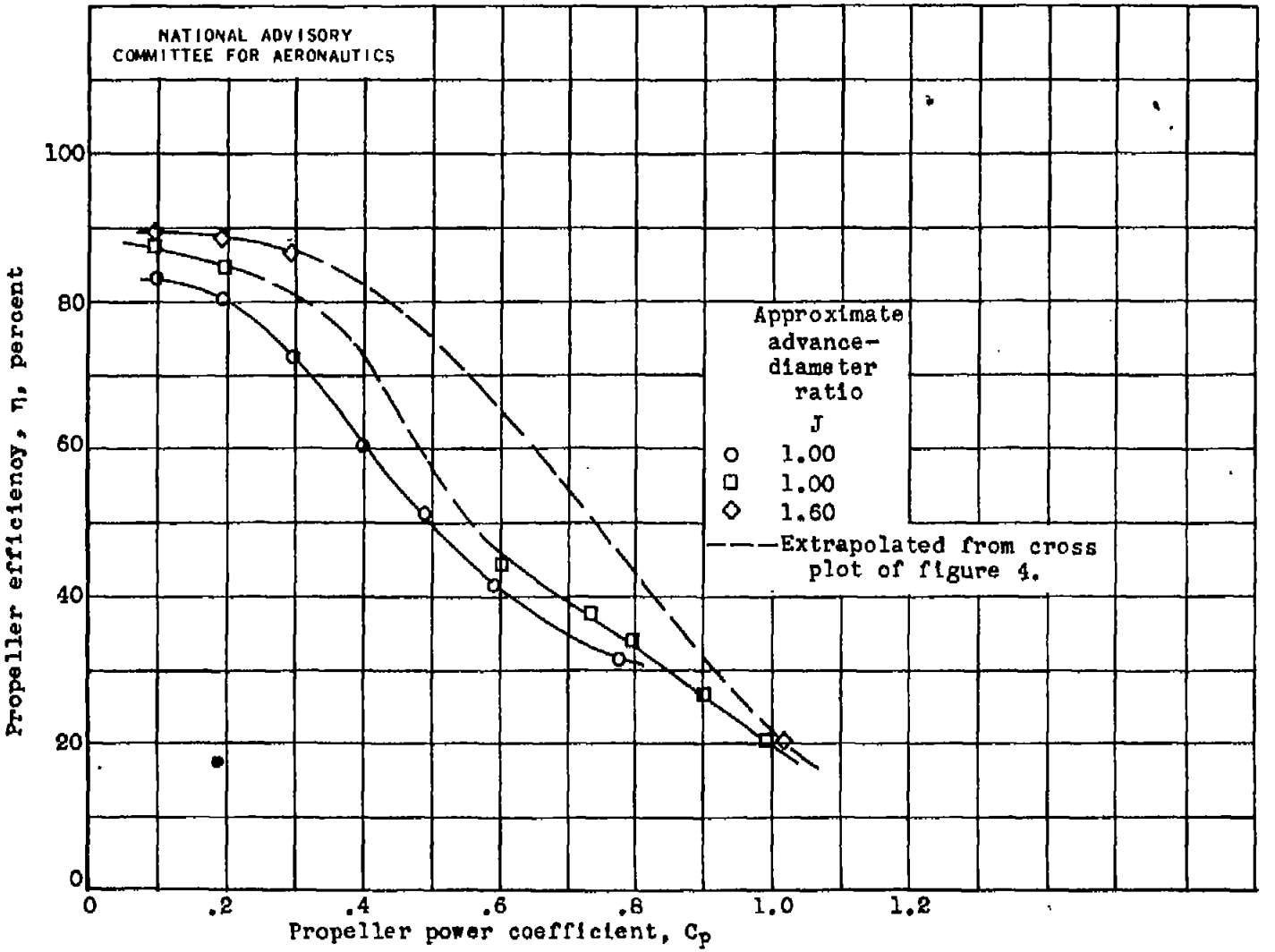

Figure 5.- Effect of power coefficient C_p on propeller efficiency η at constant advance-diameter ratio J and free-stream Mach number M_o of approximately 0.30. Curtiss 836-14C2-18R1 four-blade propeller.

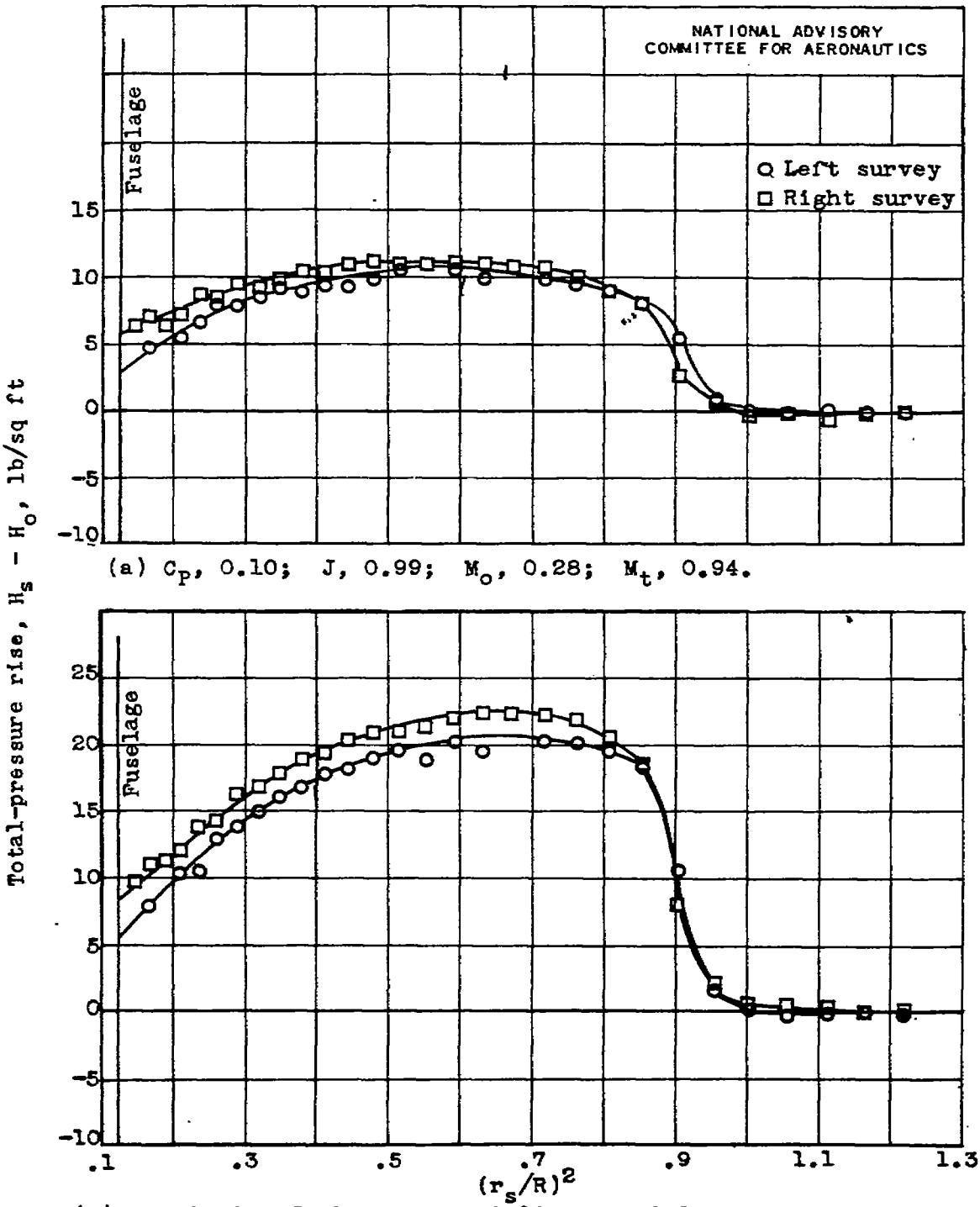

(a) C_p, 0.10; J, 0.99; M_o, 0.28; M_t, 0.94.

(b) C_p, 0.20; J, 1.00; M_o, 0.29; M_t, 0.94.

Figure 6.- Effect of power coefficient C_p on blade thrust load distribution at advance-diameter ratio J of approximately 1.00 and free-stream Mach number M_o of approximately 0.30. Curtiss 836-14C2-18R1 four-blade propeller.

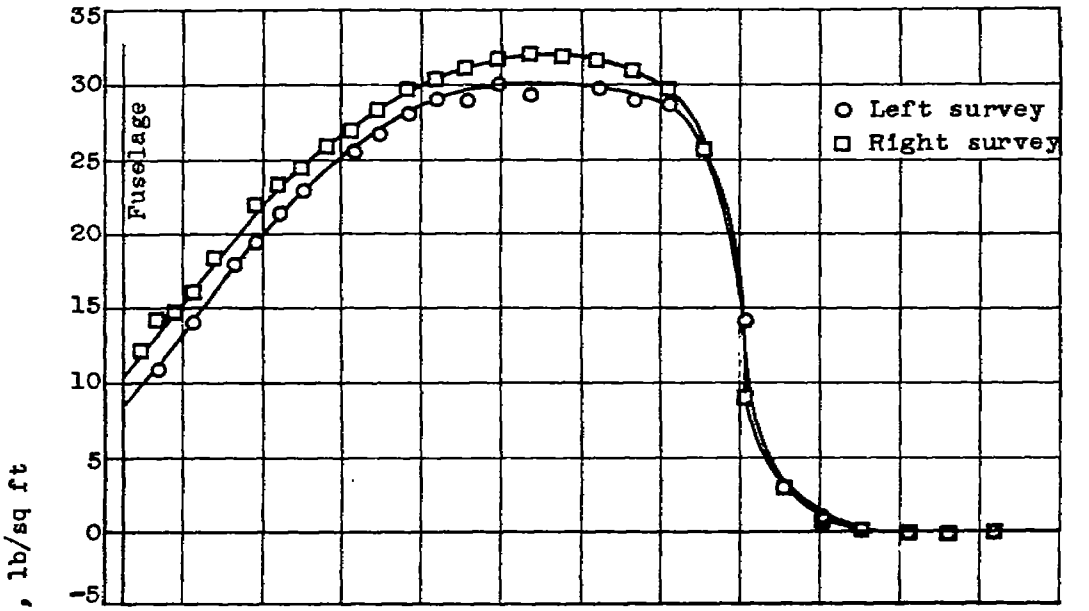

(c) C_p, 0.30; J, 1.00; M_o, 0.29; M_t, 0.94.

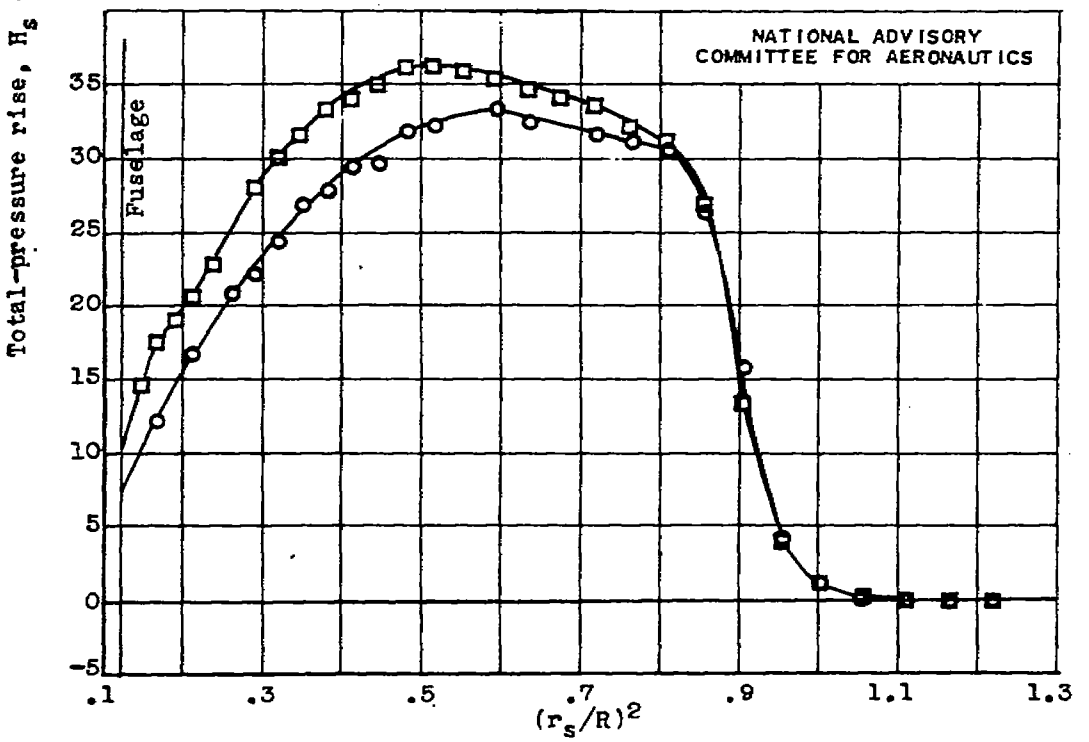

(d) C_p, 0.40; J, 1.01; M_o, 0.29; M_t, 0.94.

Figure 6.- Continued. Effect of power coefficient C_p on blade thrust load distribution at advance-diameter ratio J of approximately 1.00 and free-stream Mach number M_o of approximately 0.30. Curtiss 836-14C2-18R1 four-blade propeller.

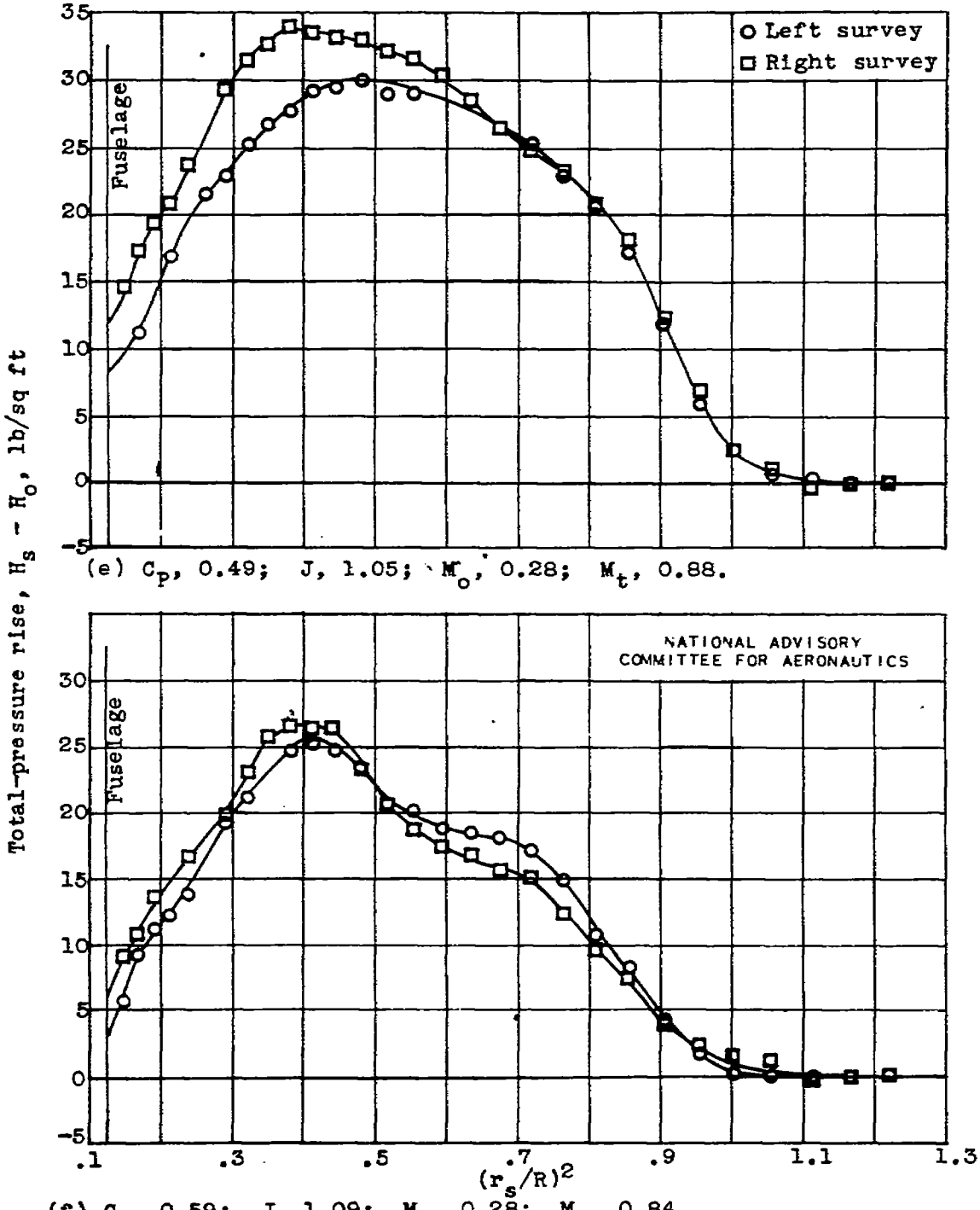

(e) C_p, 0.49; J, 1.05; M_o, 0.28; M_t, 0.88.

(f) C_p, 0.59; J, 1.09; M_o, 0.28; M_t, 0.84.

Figure 6.- Continued. Effect of power coefficient C_p on blade thrust load distribution at advance-diameter ratio J of approximately 1.00 and free-stream Mach number M_o of approximately 0.30. Curtiss 836-14C2-18R1 four-blade propeller.

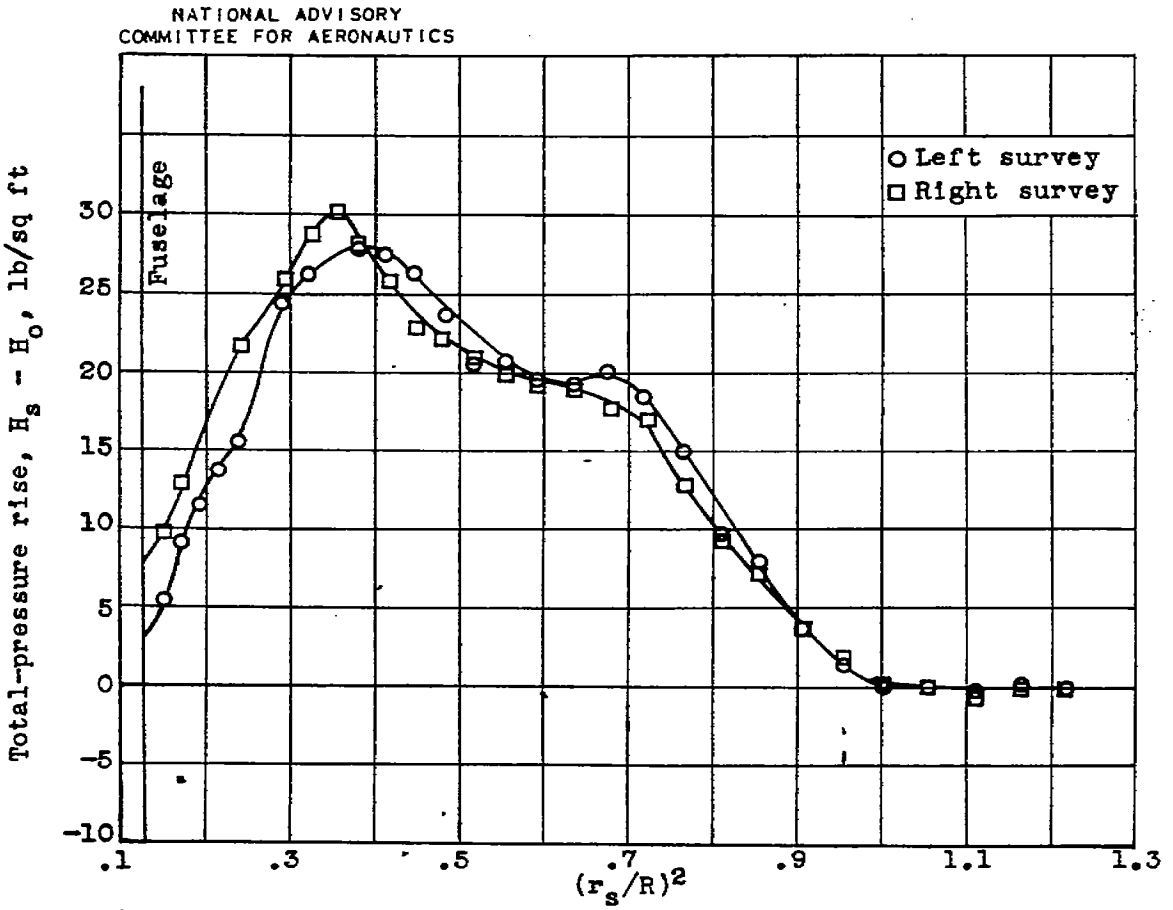

(g) C_p, 0.68; J, 1.11; M_o, 0.28; M_t, 0.85.

Figure 6.- Concluded. Effect of power coefficient C_p on blade thrust load distribution at advance-diameter ratio J of approximately 1.00 and free-stream Mach number M_o of approximately 0.30. Curtiss 836-14C2-18R1 four-blade propeller.

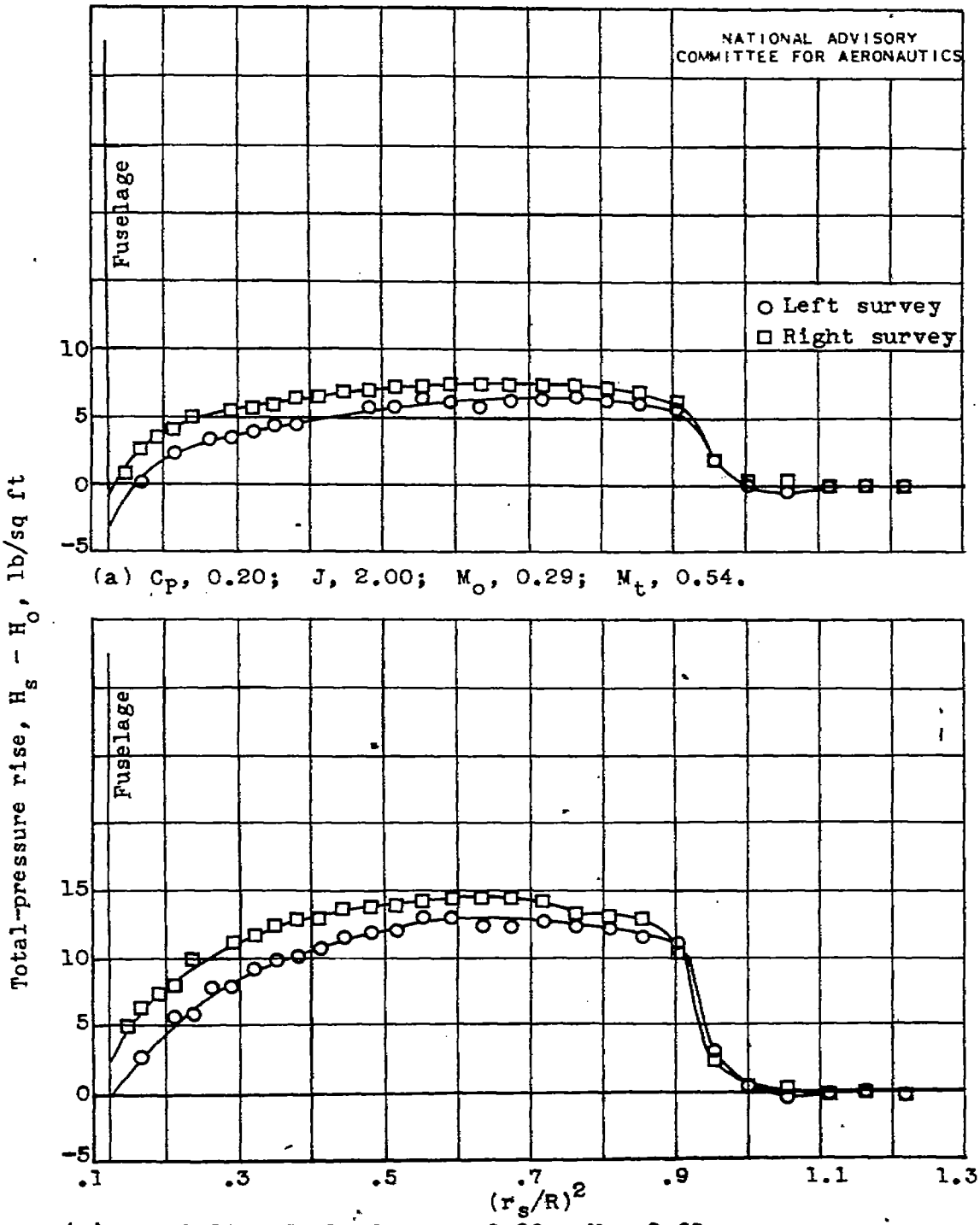

(a) C_p, 0.20; J, 2.00; M_o, 0.29; M_t, 0.54.

(b) C_p, 0.20; J, 1.59; M_o, 0.29; M_t, 0.65.

Figure 7.- Effect of advance-diameter ratio J on blade thrust load distribution at power coefficient C_p of approximately 0.20 and free-stream Mach number M_o of approximately 0.30. Curtiss 836-14C2-18R1 four-blade propeller.

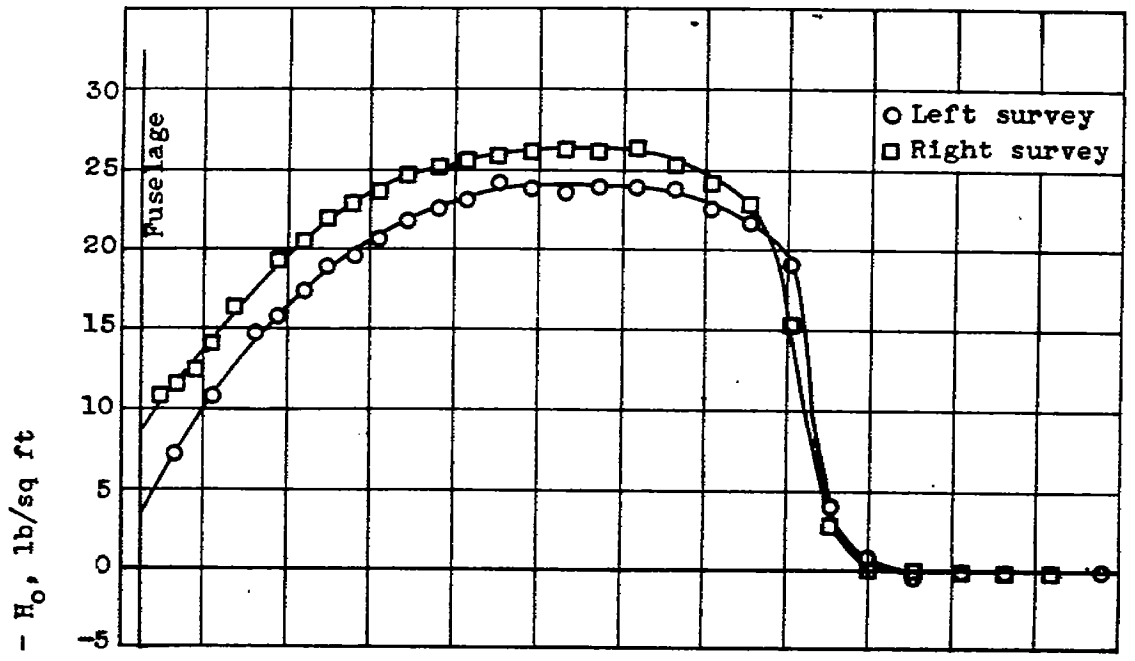

(c) C_p, 0.19; J, 1.32; M_o, 0.30; M_t, 0.78.

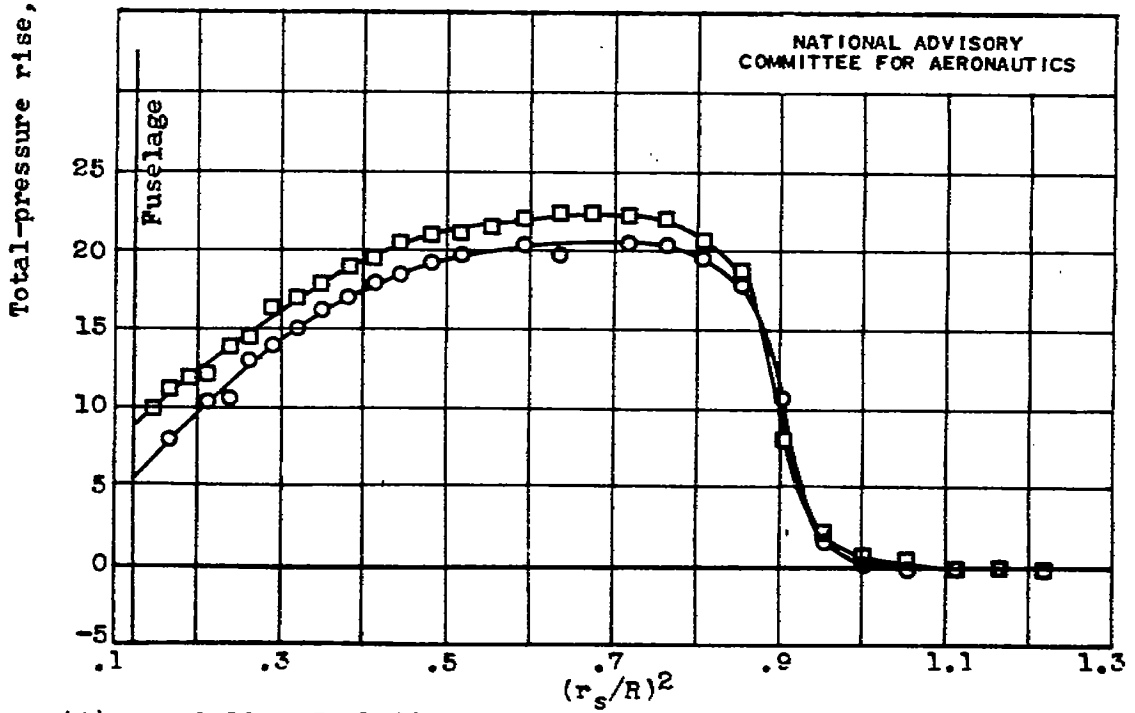

(d) C_p, 0.20; J, 1.00; M_o, 0.29; M_t, 0.94.

Figure 7.- Concluded. Effect of advance-diameter ratio J on blade thrust load distribution at power coefficient C_p of approximately 0.20 and free-stream Mach number M_o of approximately 0.30. Curtiss 836-14C2-18R1 four-blade propeller.

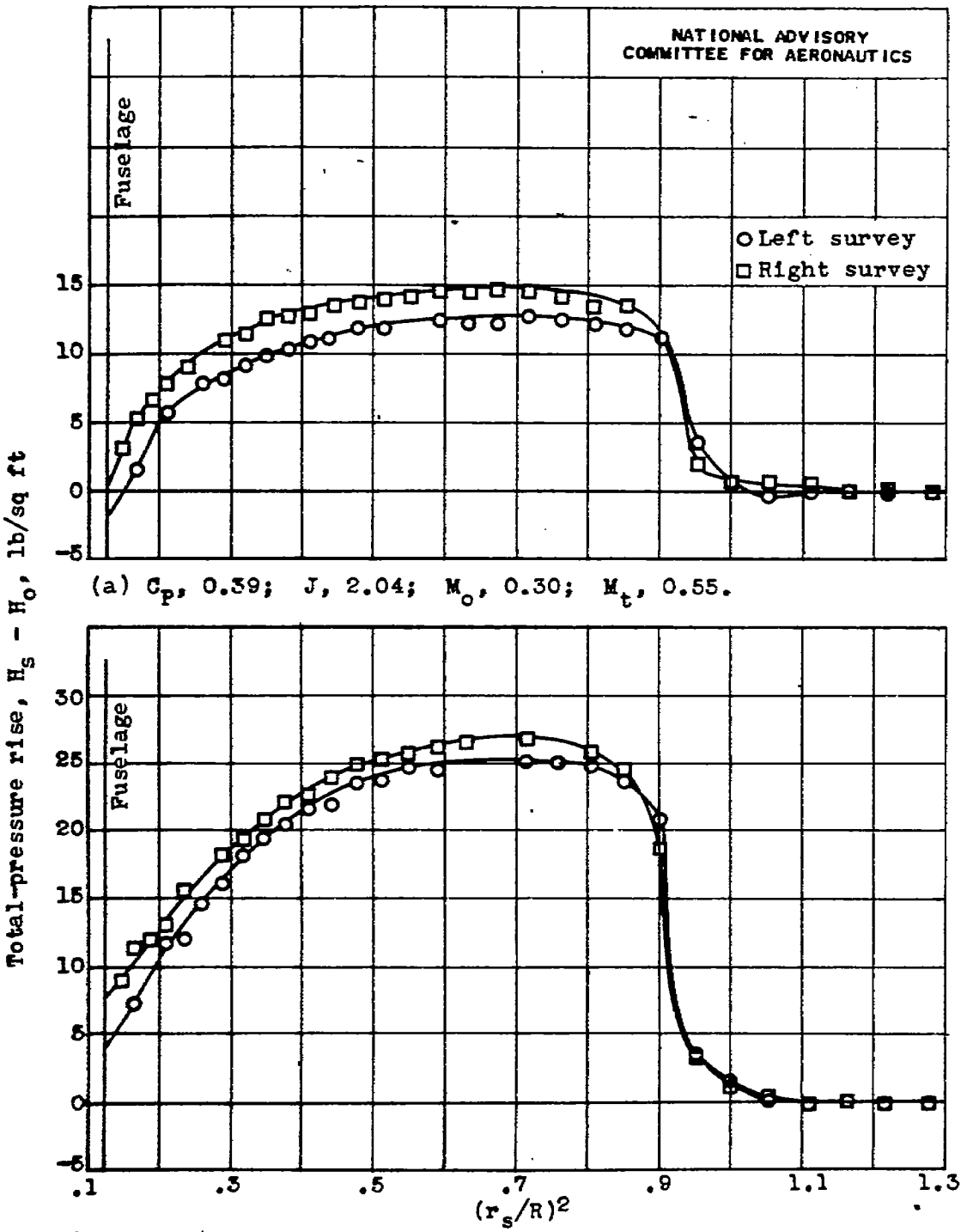

(a) C_p, 0.39; J, 2.04; M_o, 0.30; M_t, 0.55.

(b) C_p, 0.39; J, 1.16; M_o, 0.28; M_t, 0.82.

Figure 8.- Effect of advance-diameter ratio J on blade thrust load distribution at power coefficient C_p of approximately 0.40 and free-stream Mach number M_o of approximately 0.30. Curtiss 836-14C2-18R1 four-blade propeller.

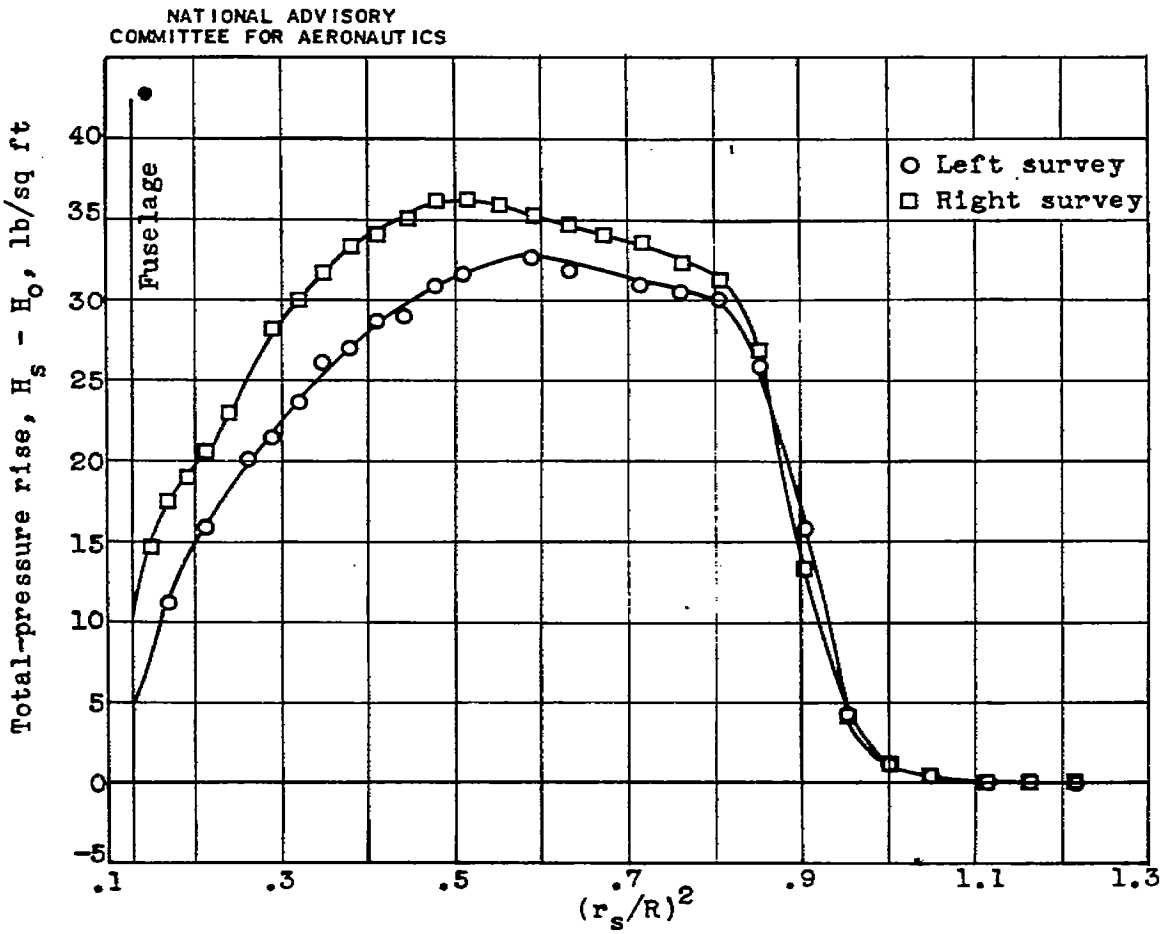

(c) C_p, 0.40; J, 1.01; M_o, 0.29; M_t, 0.94.

Figure 8.- Concluded. Effect of advance-diameter ratio J on blade thrust load distribution at power coefficient C_p of approximately 0.40 and free-stream Mach number M_o of approximately 0.30. Curtiss 836-14C2-18R1 four-blade propeller.

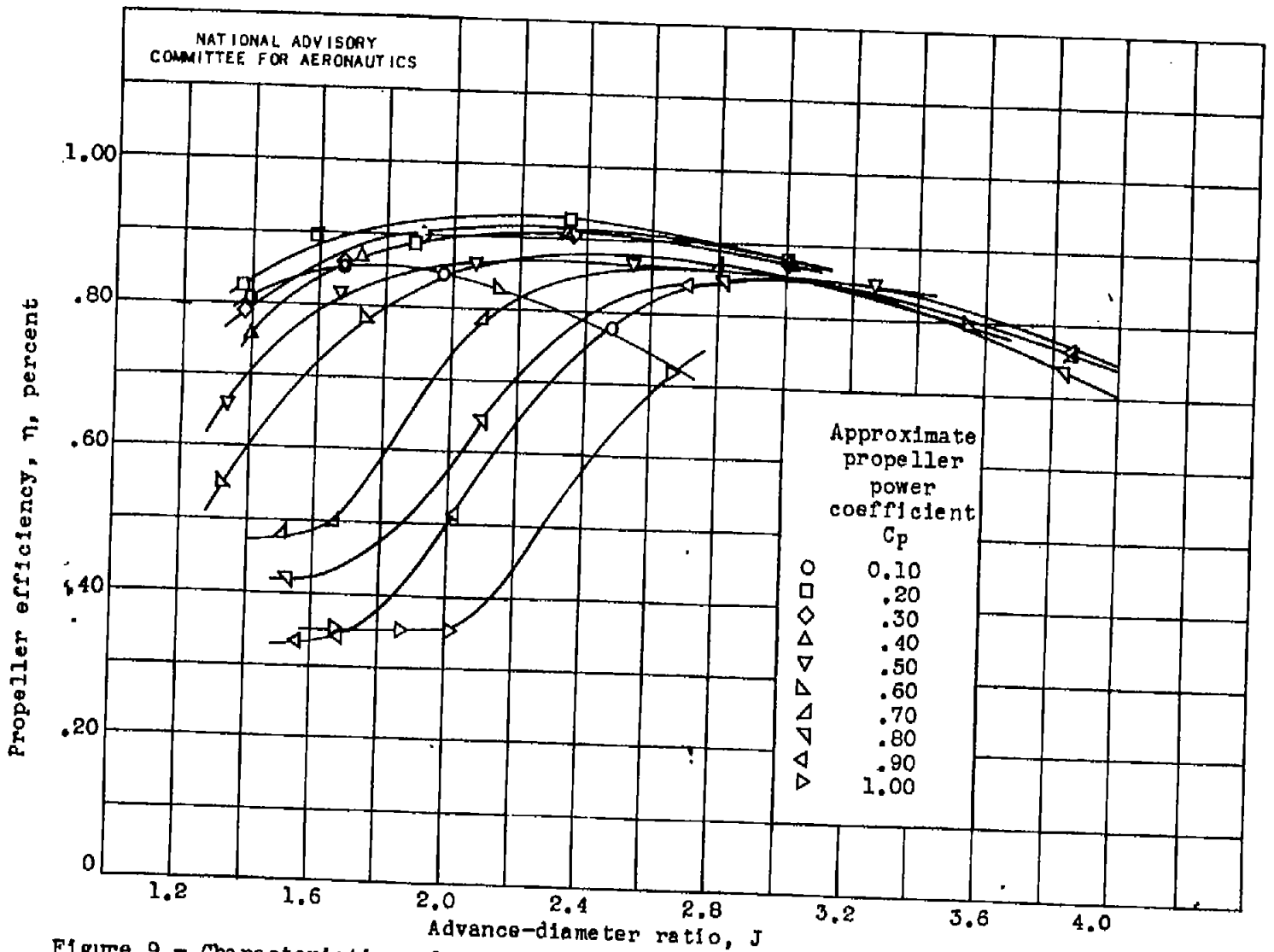

Figure 9.- Characteristics of Curtiss 836-14C2-18R1 four-blade propeller on YP-47M airplane at free-stream Mach number M_o of approximately 0.40.

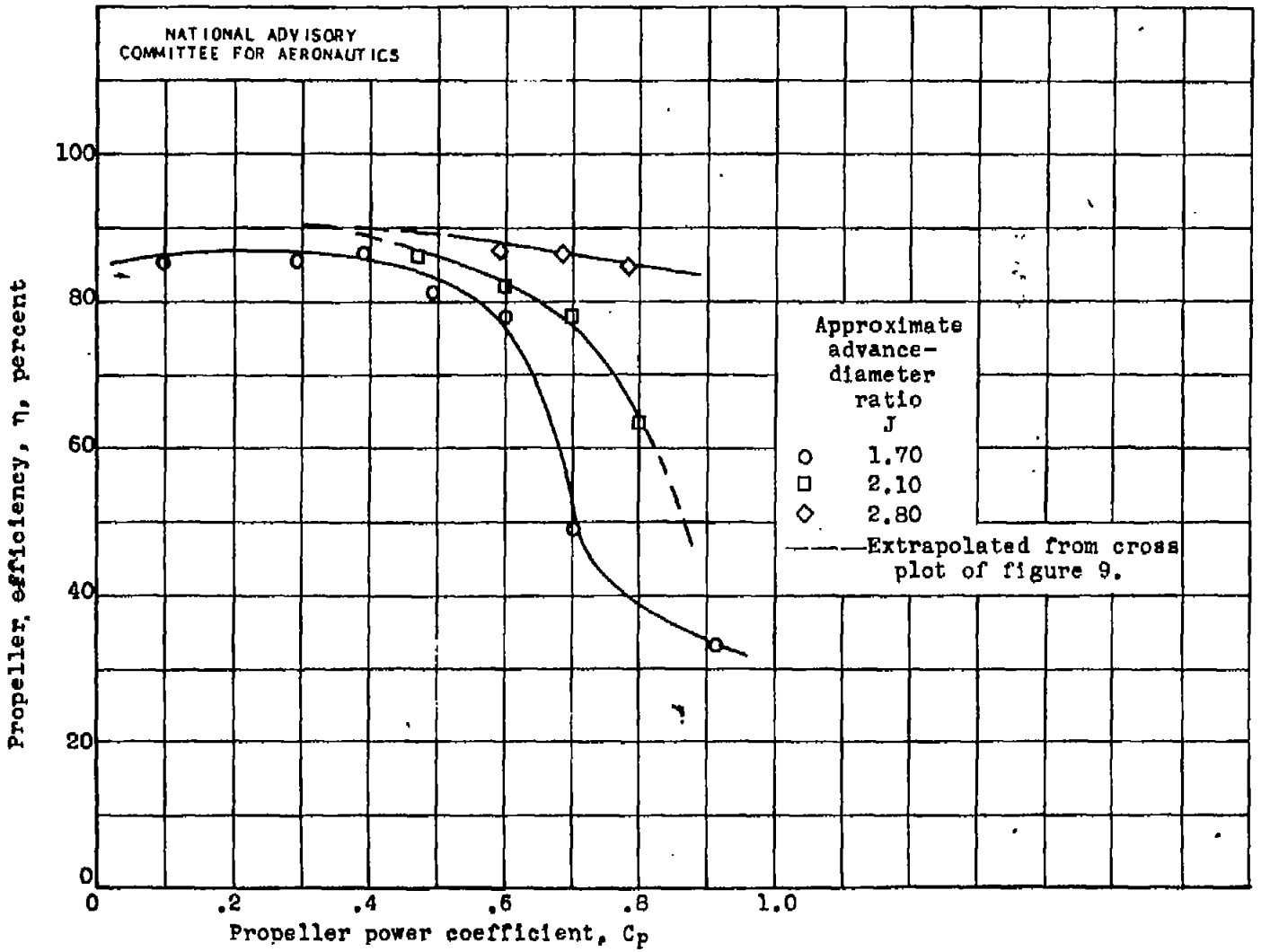

Figure 10.- Effect of power coefficient C_p on propeller efficiency η at constant advance-diameter ratio J and free-stream Mach number M_o of 0.40. Curtiss 836-14C2-18R1 four-blade propeller.

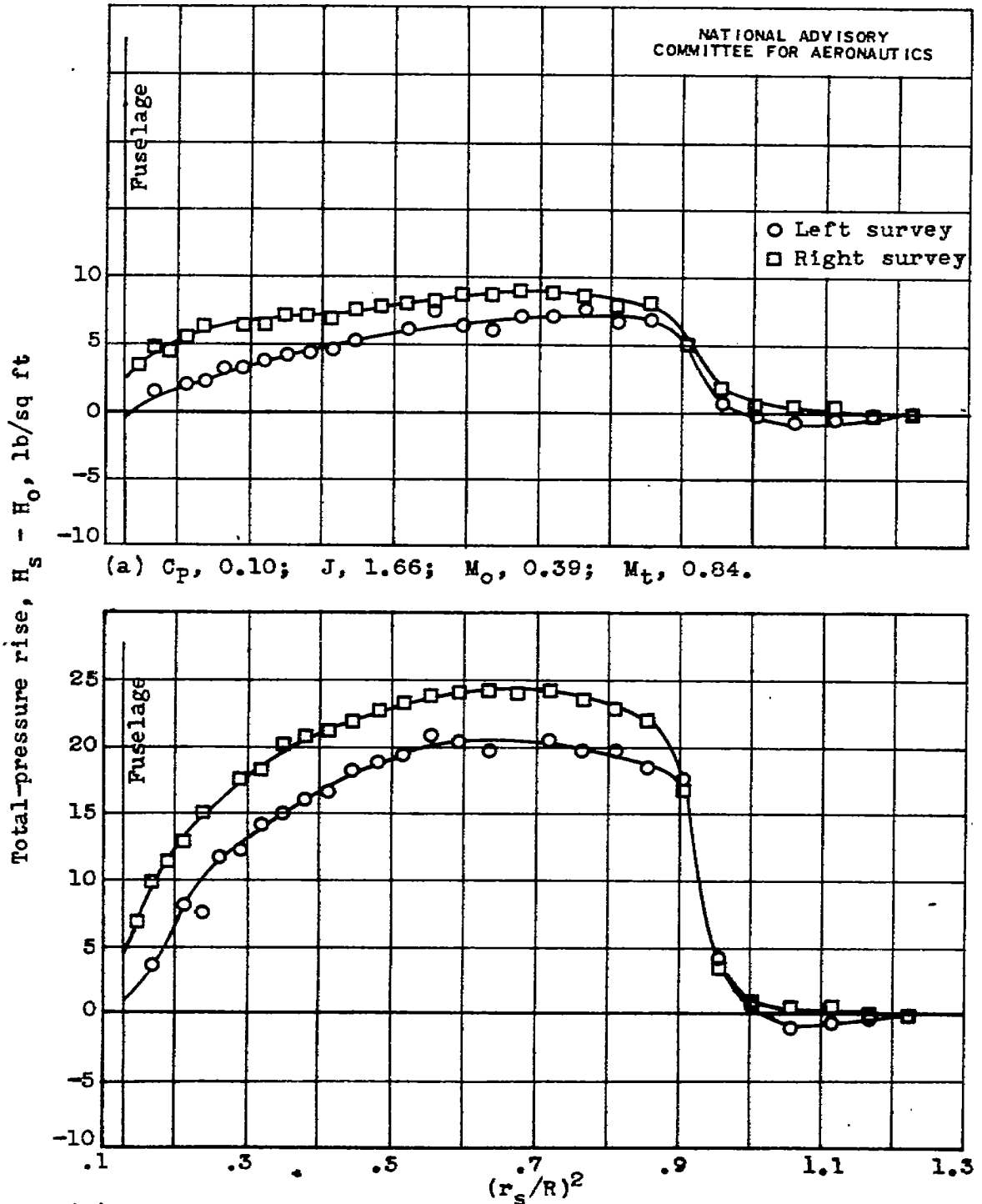

(a) C_p, 0.10; J, 1.66; M_o, 0.39; M_t, 0.84.

(b) C_p, 0.30; J, 1.67; M_o, 0.40; M_t, 0.84.

Figure 11.- Effect of power coefficient C_p on blade thrust load distribution at advance-diameter ratio J of approximately 1.70 and free-stream Mach number M_o of approximately 0.40. Curtiss 836-14C2-18R1 four-blade propeller.

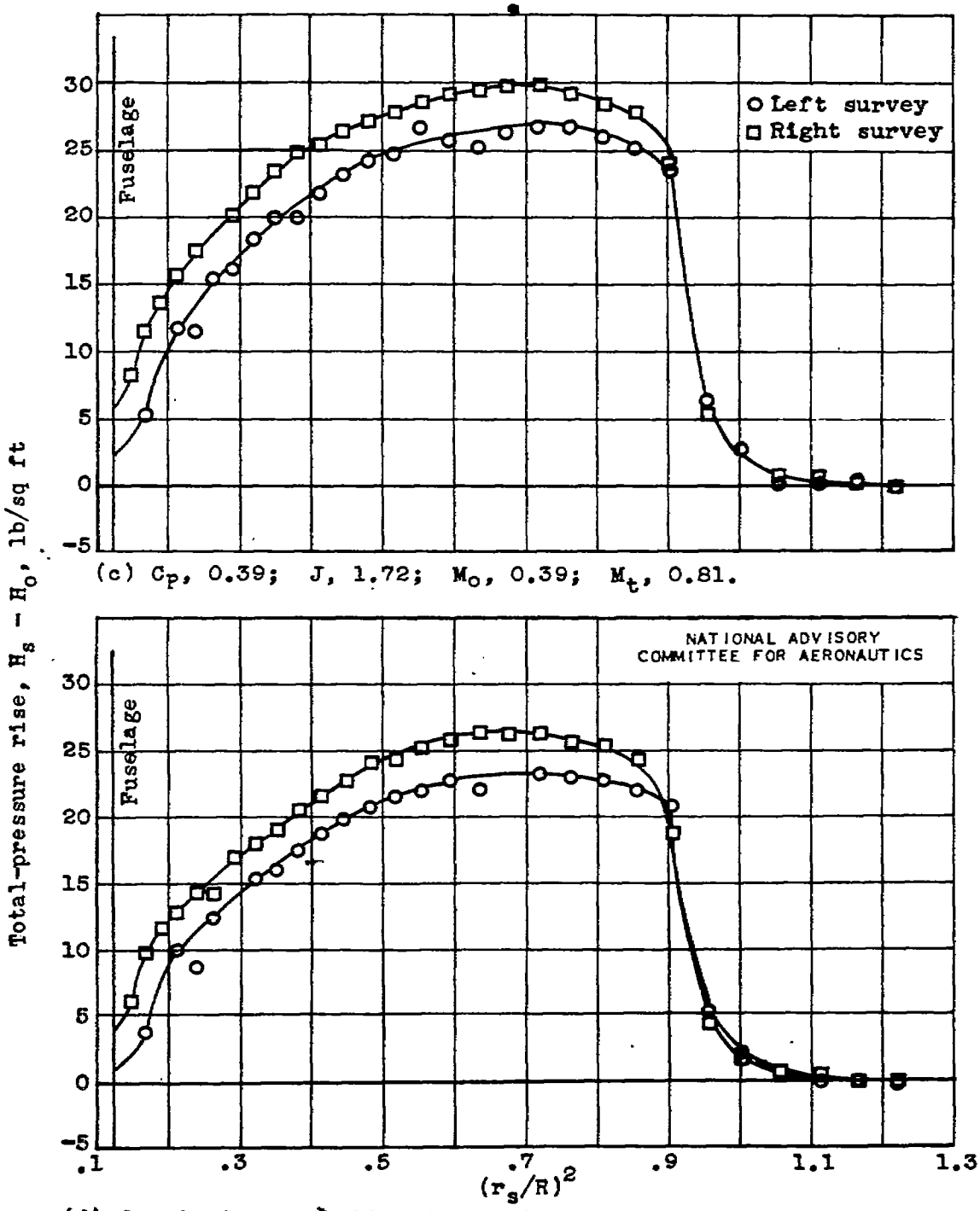

(c) C_p, 0.39; J, 1.72; M_o, 0.39; M_t, 0.81.

(d) C_p, 0.50; J, 1.66; M_o, 0.39; M_t, 0.83.

Figure 11.- Continued. Effect of power coefficient C_p on blade thrust load distribution at advance-diameter ratio J of approximately 1.70 and free-stream Mach number M_o of approximately 0.40. Curtiss 836-14C2-18R1 four-blade propeller.

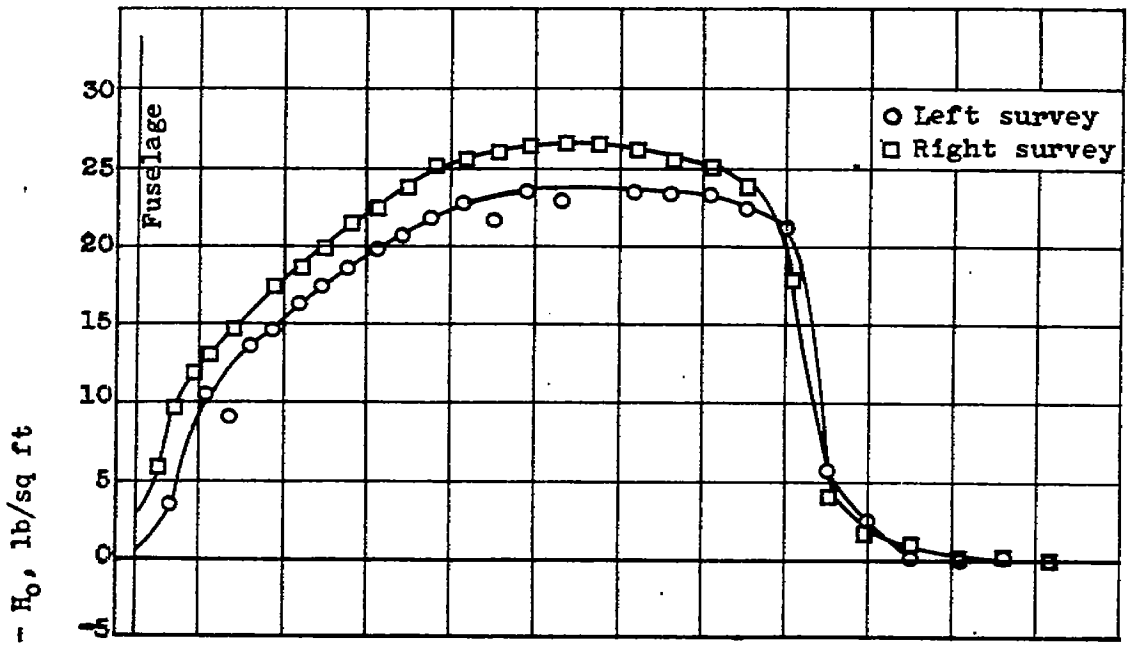

(e) C_p, 0.60; J, 1.73; M_o, 0.39; M_t, 0.81.

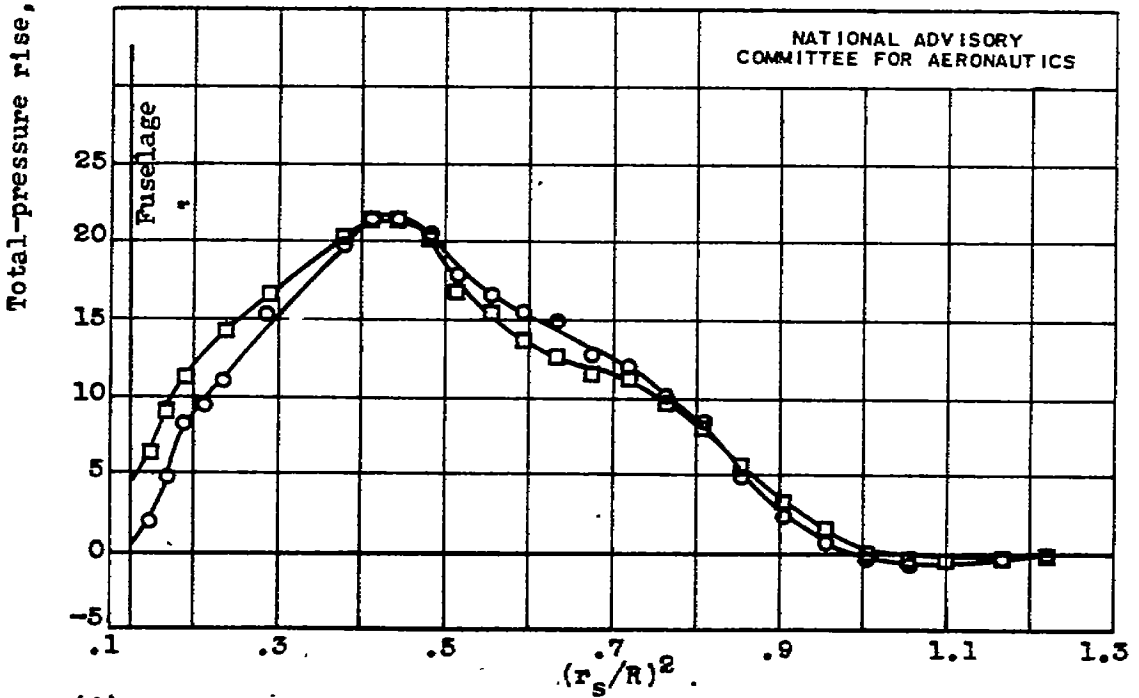

(f) C_p, 0.71; J, 1.65; M_o, 0.37; M_t, 0.80.

Figure 11.- Continued. Effect of power coefficient C_p on blade thrust load distribution at advance-diameter ratio J of approximately 1.70 and free-stream Mach number M_o of approximately 0.40. Curtiss 836-14C2-18R1 four-blade propeller.

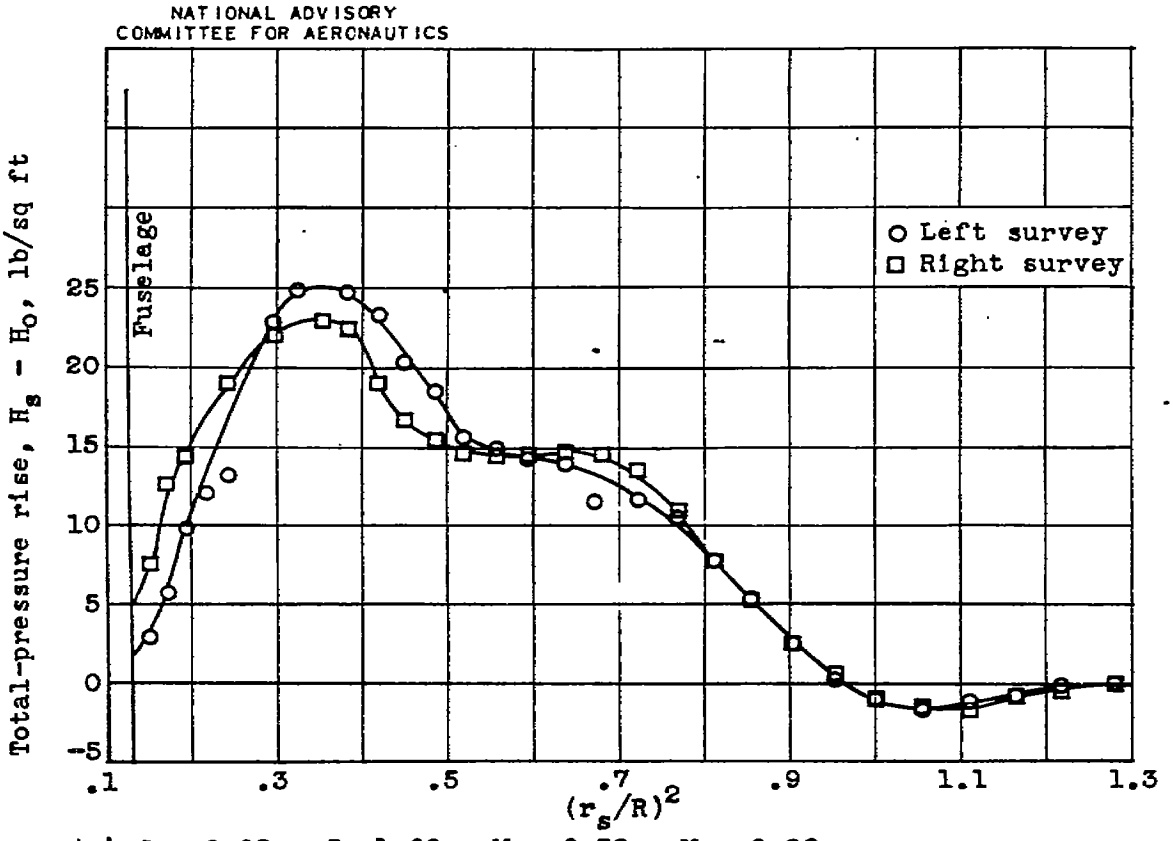

(g) C_p, 0.92; J, 1.68; M_o, 0.38; M_t, 0.80.

Figure 11.- Concluded. Effect of power coefficient C_p on blade thrust load distribution at advance-diameter ratio J of approximately 1.70 and free-stream Mach number M_o of approximately 0.40. Curtiss 836-14C2-18R1 four-blade propeller.

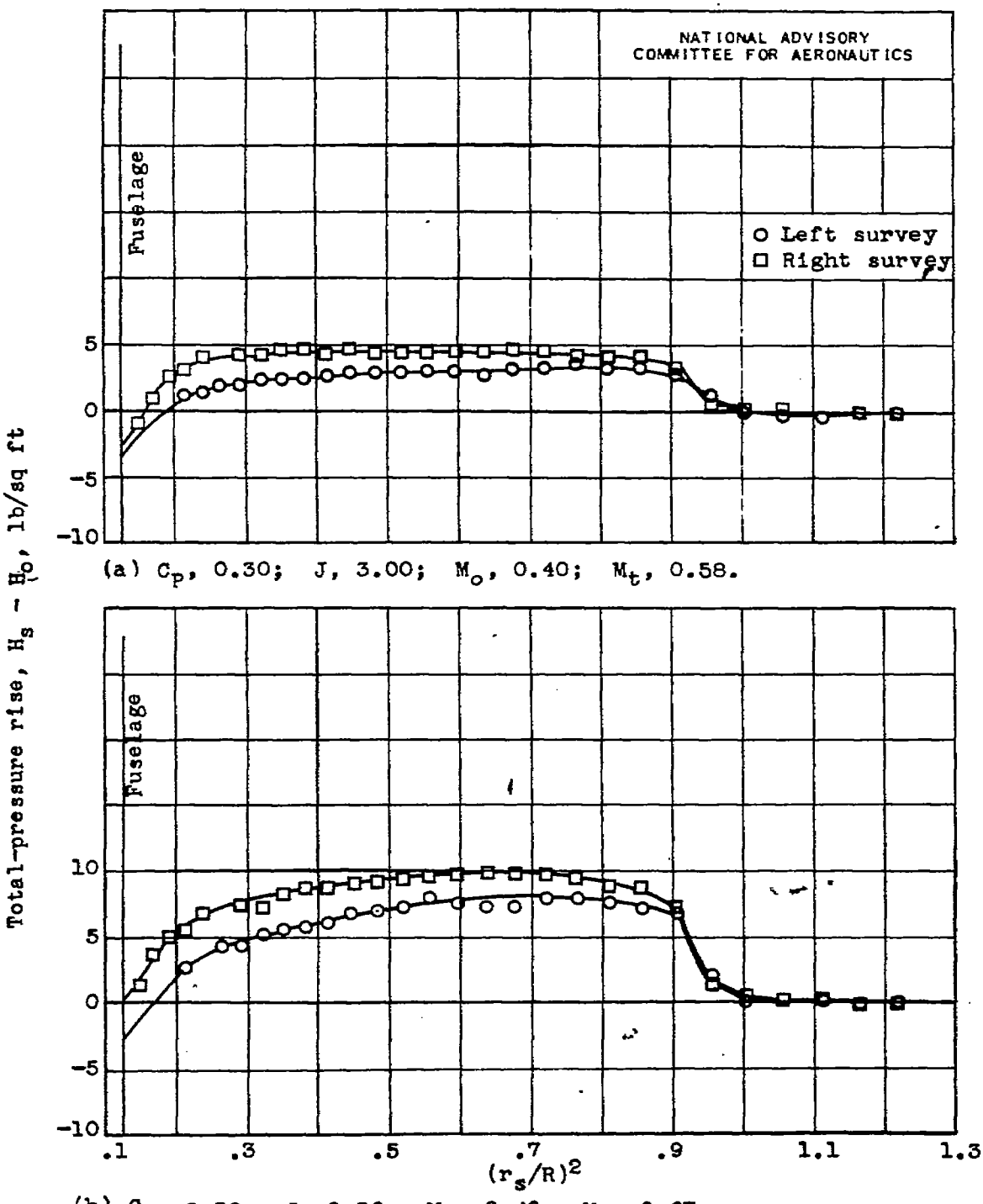

(a) C_p, 0.30; J, 3.00; M_o, 0.40; M_t, 0.58.

(b) C_p, 0.30; J, 2.36; M_o, 0.40; M_t, 0.67.

Figure 12.- Effect of advance-diameter ratio J on blade thrust load distribution at power coefficient C_p of approximately 0.30 and free-stream Mach number M_o of approximately 0.40. Curtiss 836-14C2-18R1 four-blade propeller.

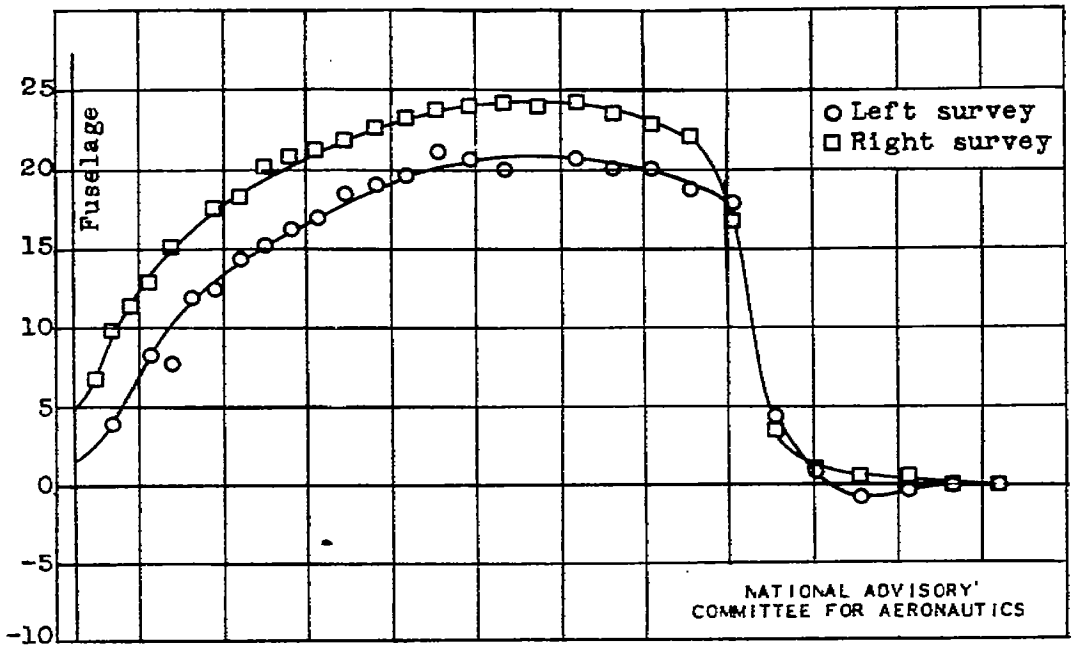

(c) C_p, 0.29; J, 1.67; M_o, 0.40; M_t, 0.84.

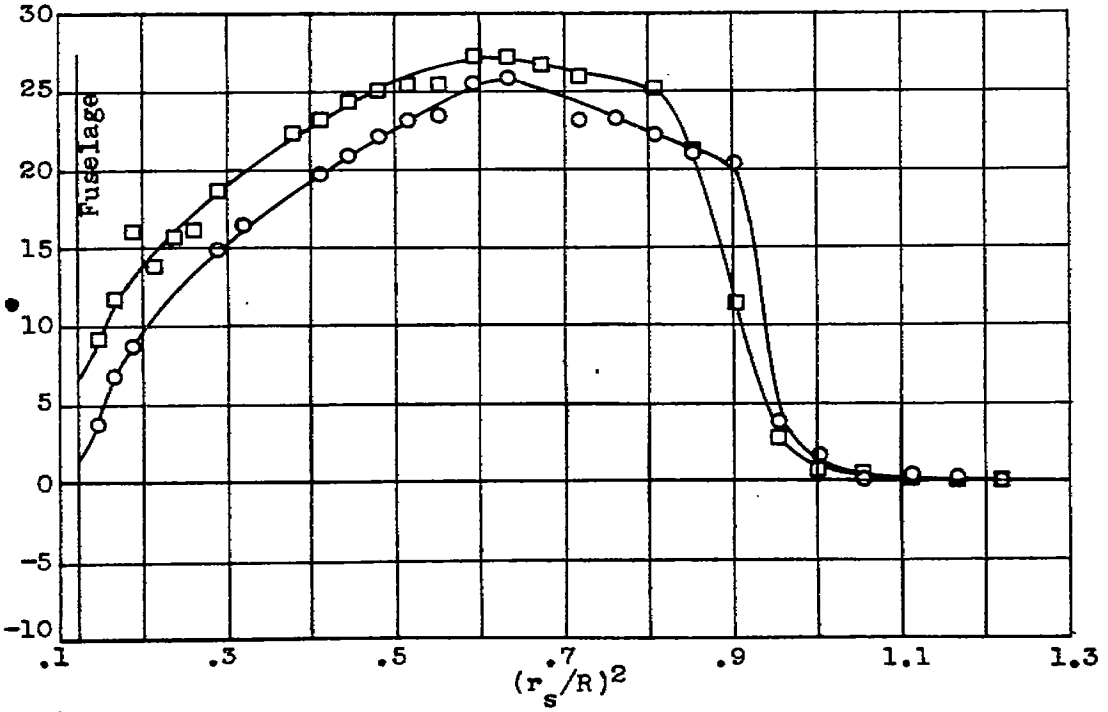

Total-pressure rise, $H_s - H_o$, lb/sq ft

(d) C_p, 0.30; J, 1.38; M_o, 0.39; M_t, 0.98.

Figure 12.- Concluded. Effect of advance-diameter ratio J on blade thrust load distribution at power coefficient C_p of approximately 0.30 and free-stream Mach number M_o of approximately 0.40. Curtiss 836-14C2-18R1 four-blade propeller.

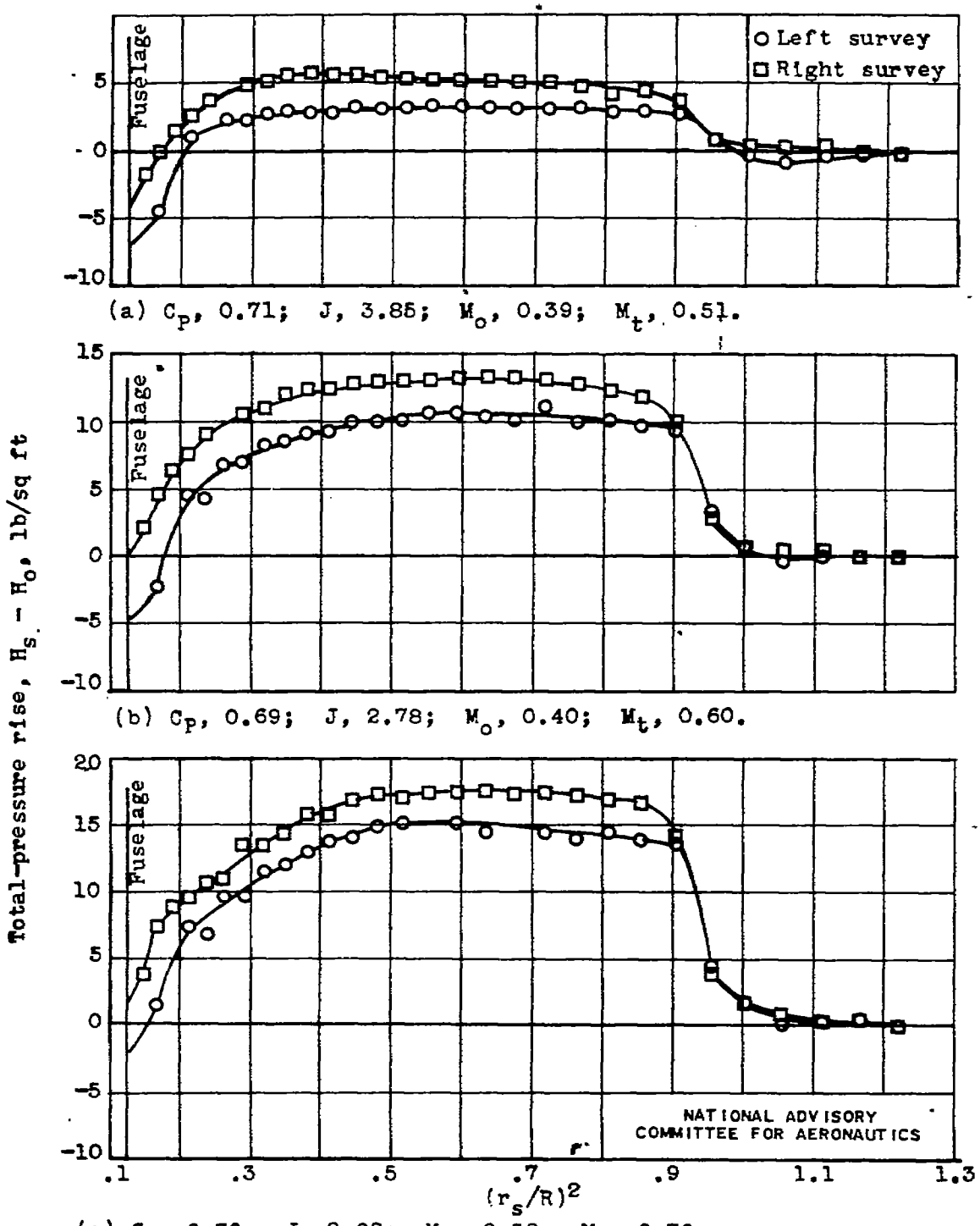

(a) C_p, 0.71; J, 3.85; M_o, 0.39; M_t, 0.51.

(b) C_p, 0.69; J, 2.78; M_o, 0.40; M_t, 0.60.

(c) C_p, 0.70; J, 2.09; M_o, 0.39; M_t, 0.70.

Figure 13.- Effect of advance-diameter ratio J on blade thrust load distribution at power coefficient C_p of approximately 0.70 and free-stream Mach number M_o of approximately 0.40. Curtiss 836-14C2-18R1 four-blade propeller.

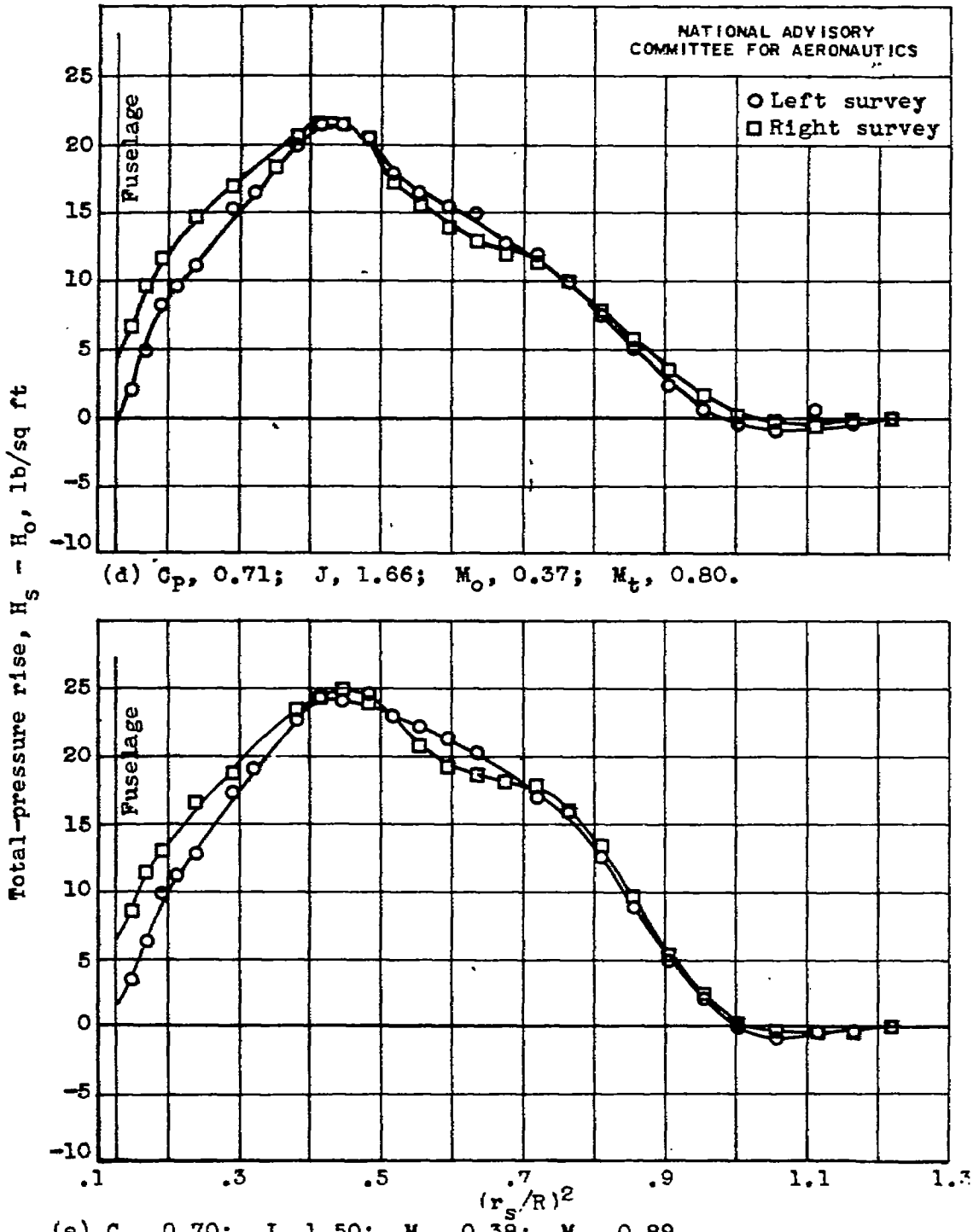

(d) C_p, 0.71; J, 1.66; M_o, 0.37; M_t, 0.80.

(e) C_p, 0.70; J, 1.50; M_o, 0.38; M_t, 0.89.

Figure 13.- Concluded. Effect of advance-diameter ratio J on blade thrust load distribution at power coefficient C_p of approximately 0.70 and free-stream Mach number M_o of approximately 0.40. Curtiss 836-1402-18R1 four-blade propeller.

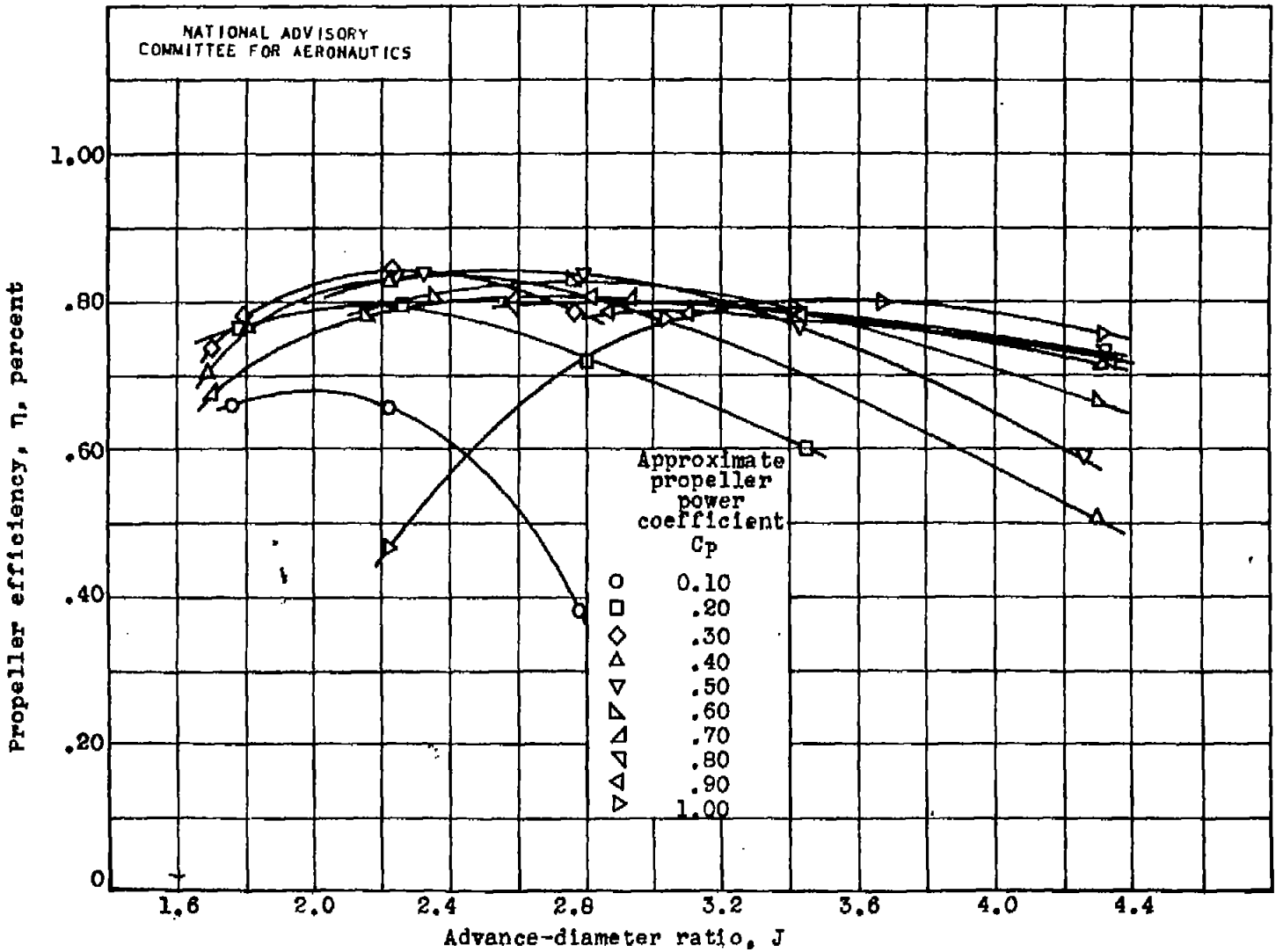

Figure 14.- Characteristics of Curtiss 836-14C2-18R1 four-blade propeller on YP-47M airplane at free-stream Mach number M_o of approximately 0.50.

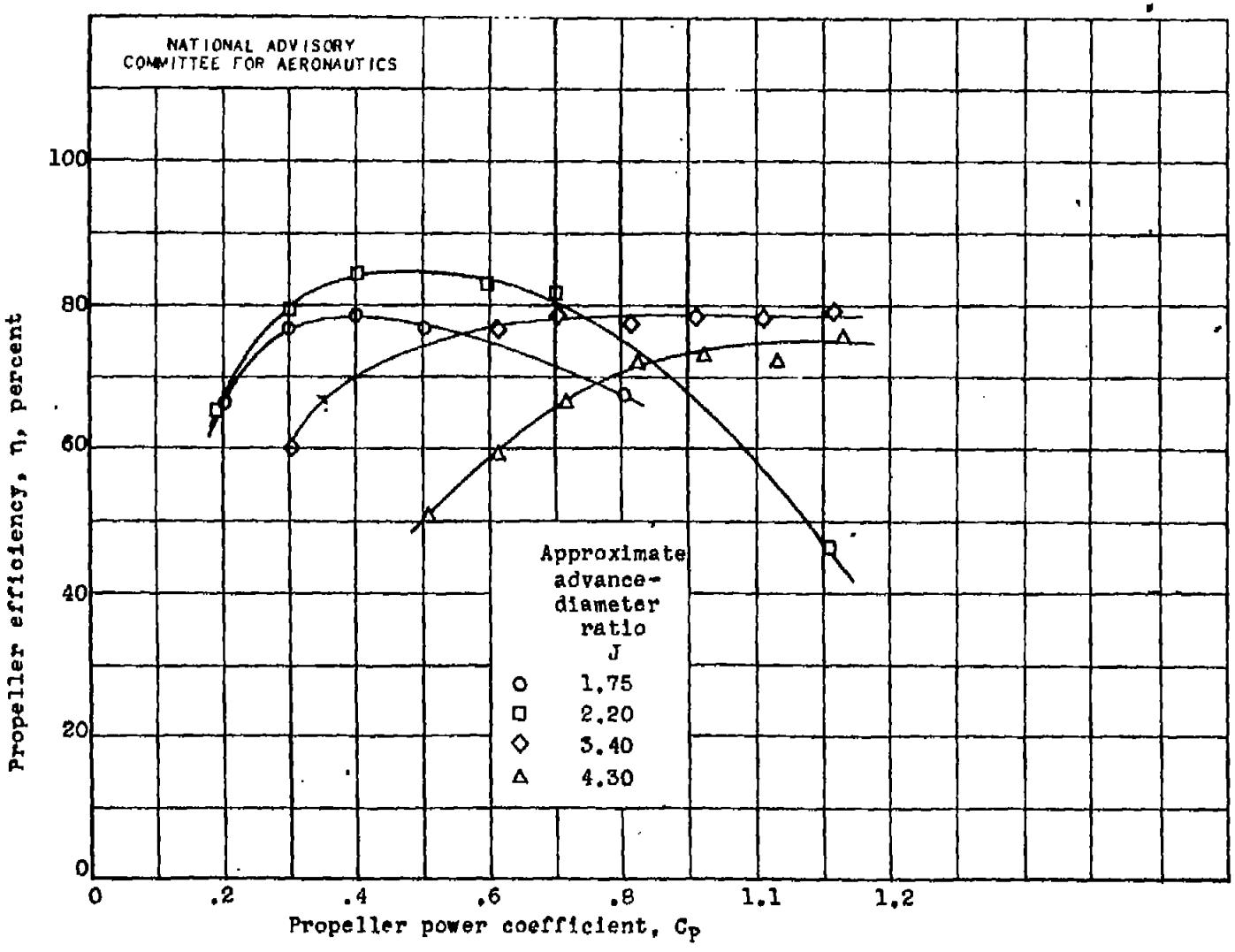

Figure 15.- Effect of power coefficient C_p on propeller efficiency η at constant advance-diameter ratio J and free-stream Mach number M_o of approximately 0.50. Curtiss 836-14C2-18R1 four-blade propeller.

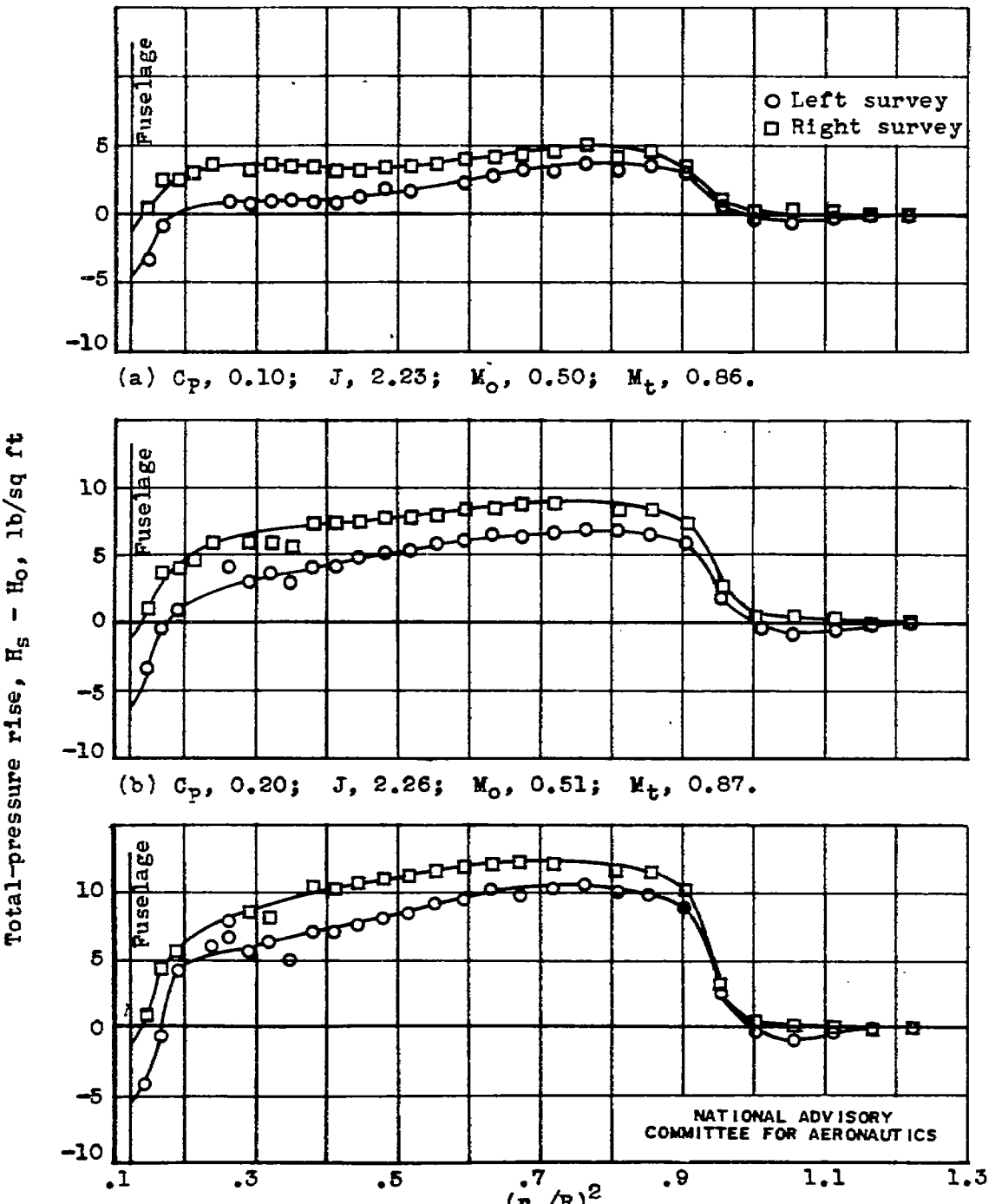

(c) C_p, 0.30; J, 2.24; M_o, 0.50; M_t, 0.86.

Figure 16.- Effect of power coefficient C_p on blade thrust load distribution at advance-diameter ratio J of approximately 2.20 and free-stream Mach number M_o of approximately 0.50. Curtiss 836-14C2-18R1 four-blade propeller.

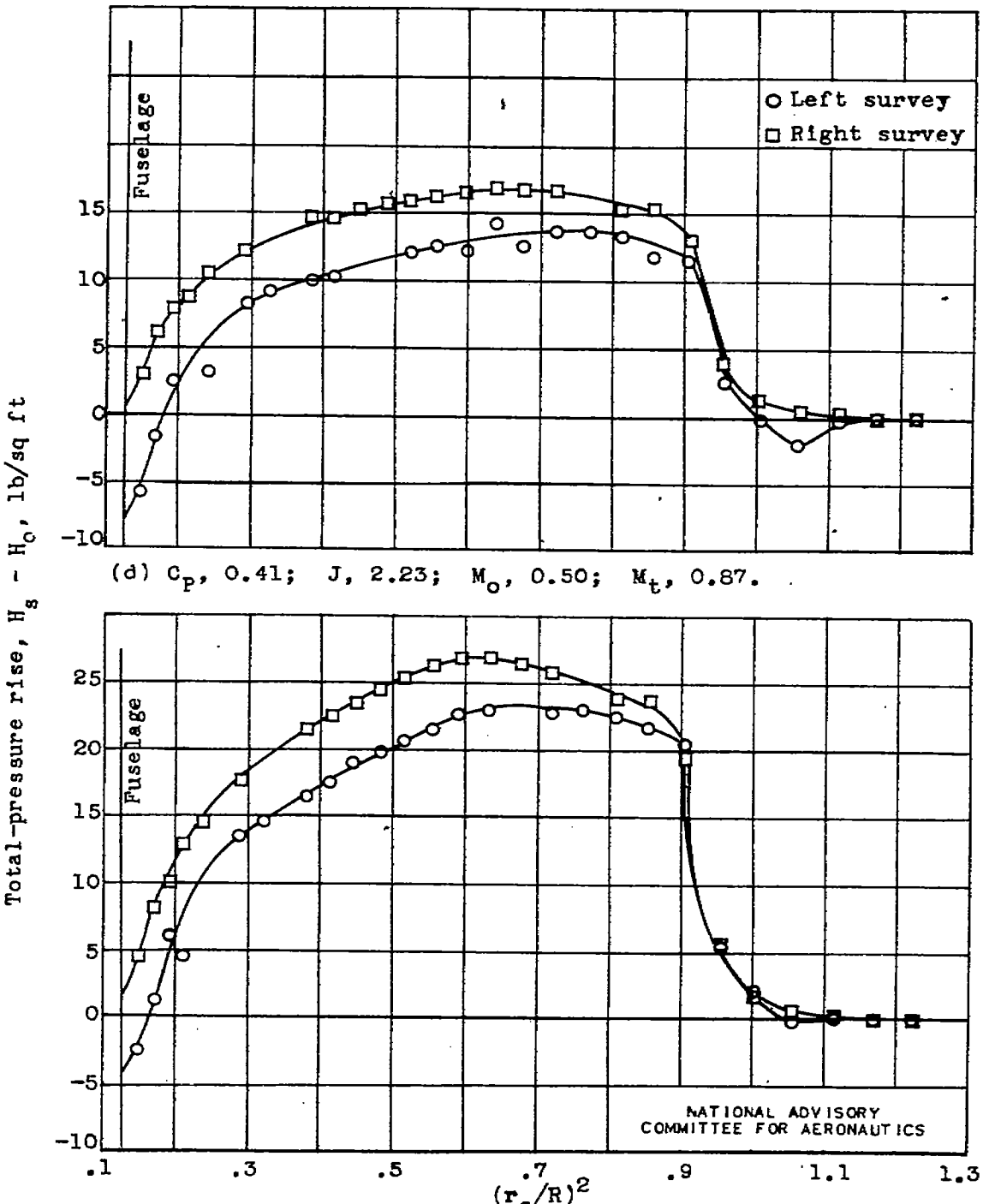

(e) C_p, 0.60; J, 2.16; M_o, 0.51; M_t, 0.89.

Figure 16.- Concluded. Effect of power coefficient C_p on blade thrust load distribution at advance-diameter ratio J of approximately 2.20 and free-stream Mach number M_o of approximately 0.50. Curtiss 836-14C2-18R1 four-blade propeller.

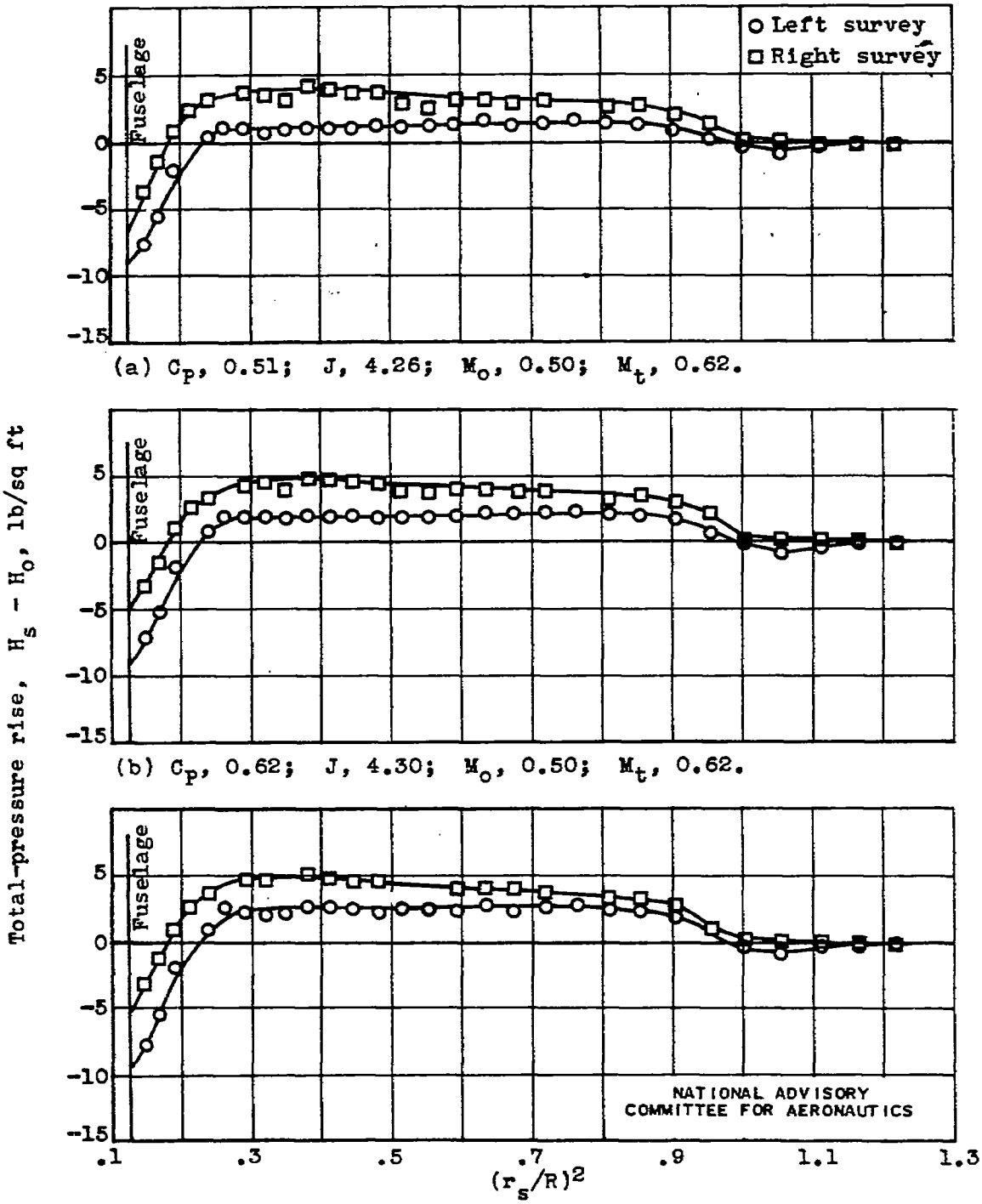

(a) C_p, 0.51; J, 4.26; M_o, 0.50; M_t, 0.62.

(b) C_p, 0.62; J, 4.30; M_o, 0.50; M_t, 0.62.

(c) C_p, 0.72; J, 4.31; M_o, 0.50; M_t, 0.63.

Figure 17.- Effect of power coefficient C_p on blade thrust load distribution at advance-diameter ratio J of approximately 4.30 and free-stream Mach number M_o of approximately 0.50. Curtiss 836-14C2-18R1 four-blade propeller.

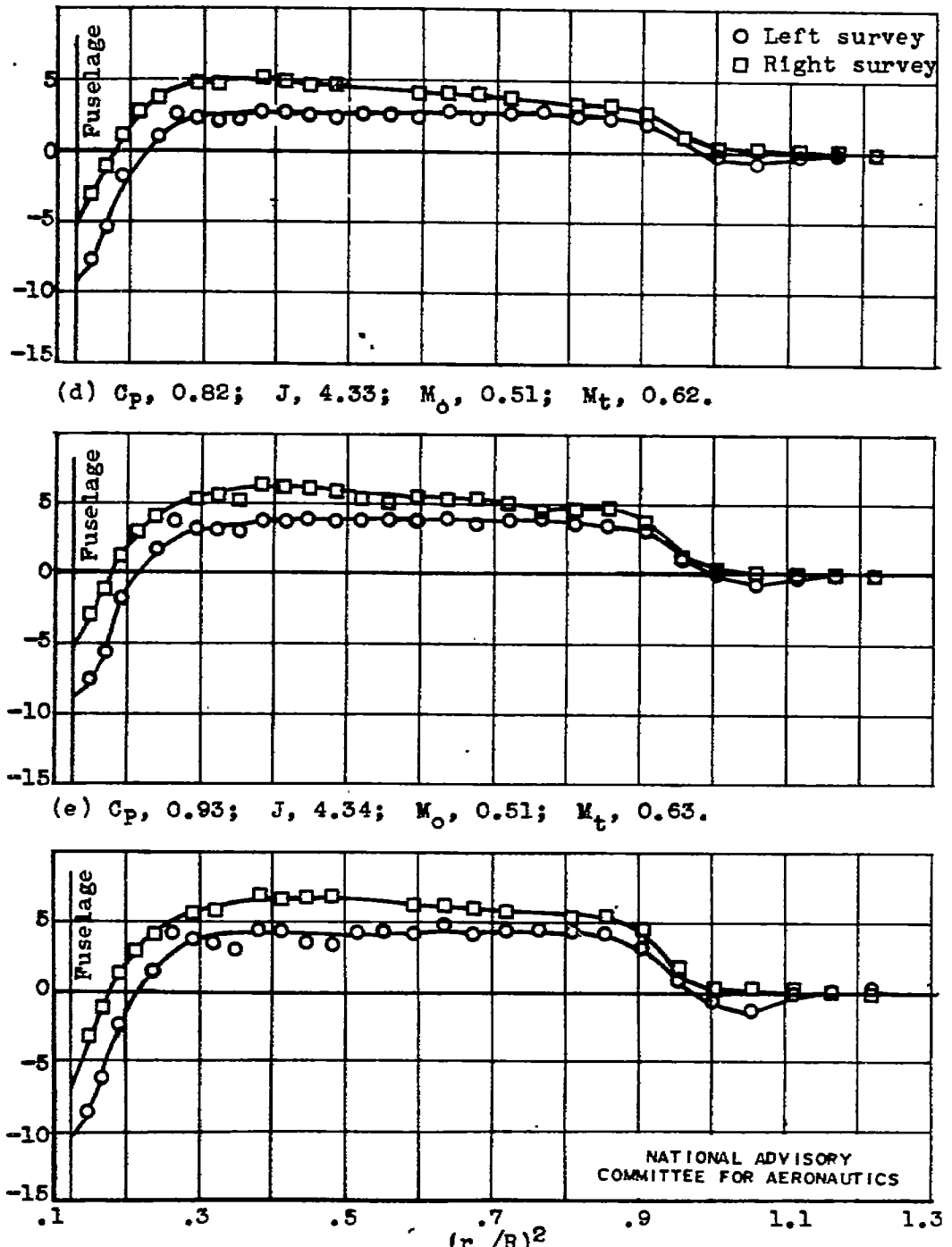

(d) C_p, 0.82; J, 4.33; M_o, 0.51; M_t, 0.62.

(e) C_p, 0.93; J, 4.34; M_o, 0.51; M_t, 0.63.

(f) C_p, 1.03; J, 4.32; M_o, 0.50; M_t, 0.62.

Figure 17.- Concluded. Effect of power coefficient C_p on blad thrust load distribution at advance-diameter ratio J of approximately 4.30 and free-stream Mach number M_o of approximately 0.50. Curtiss 836-14C2-18R1 four-blade propeller.

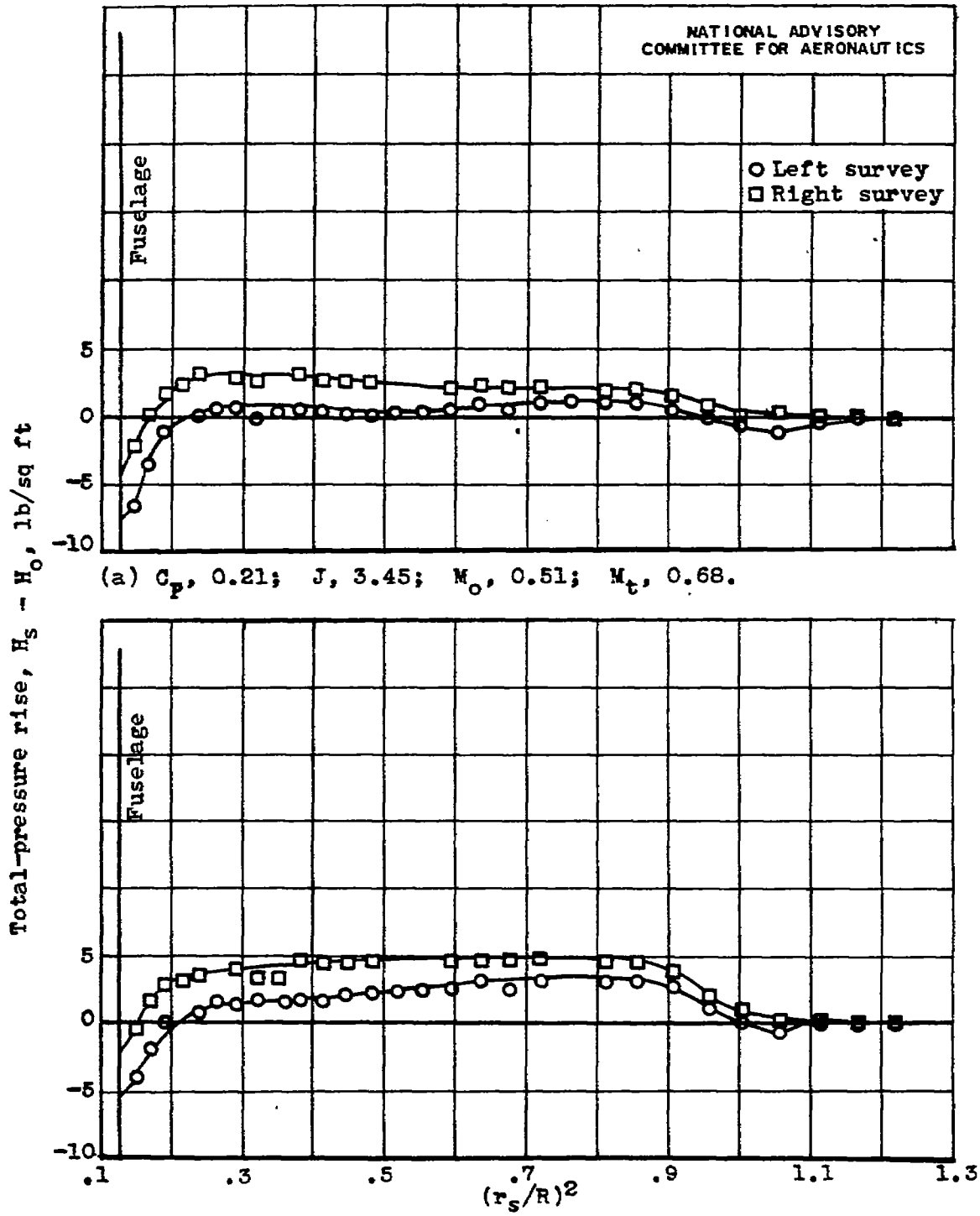

(a) C_p, 0.21; J, 3.45; M_o, 0.51; M_t, 0.68.

(b) C_p, 0.21; J, 2.81; M_o, 0.51; M_t, 0.76.

Figure 18.- Effect of advance-diameter ratio J on blade thrust load distribution at power coefficient C_p of approximately 0.20 and free-stream Mach number M_o of approximately 0.50. Curtiss 836-14C2-18R1 four-blade propeller.

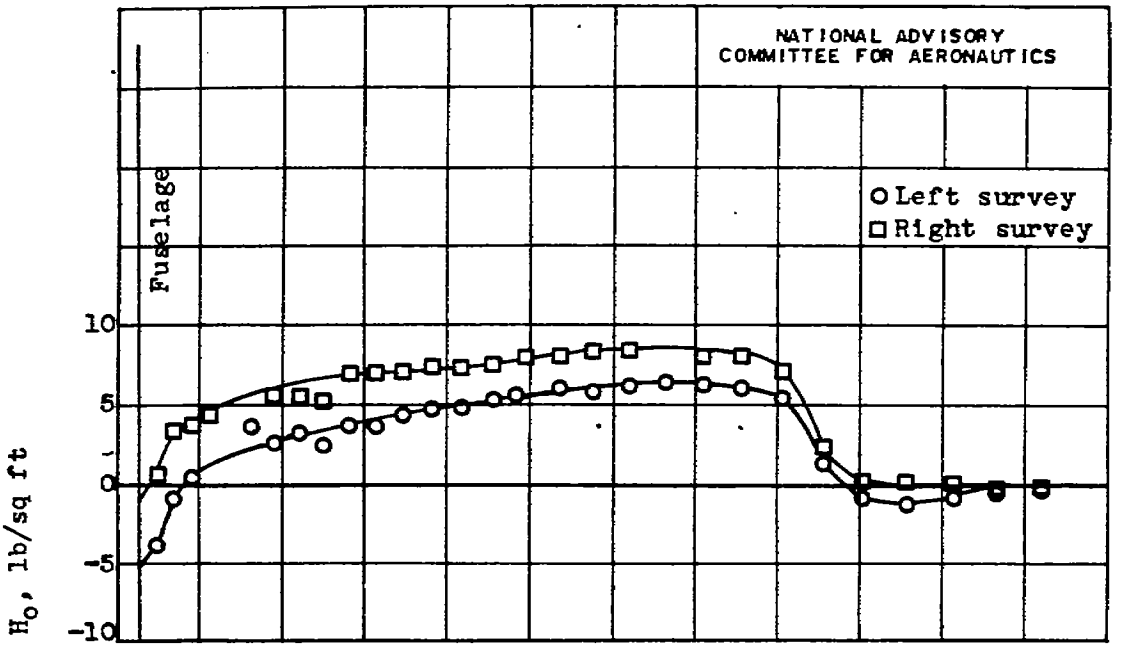

(c) C_P, 0.20; J, 2.26; M_o, 0.51; M_t, 0.87.

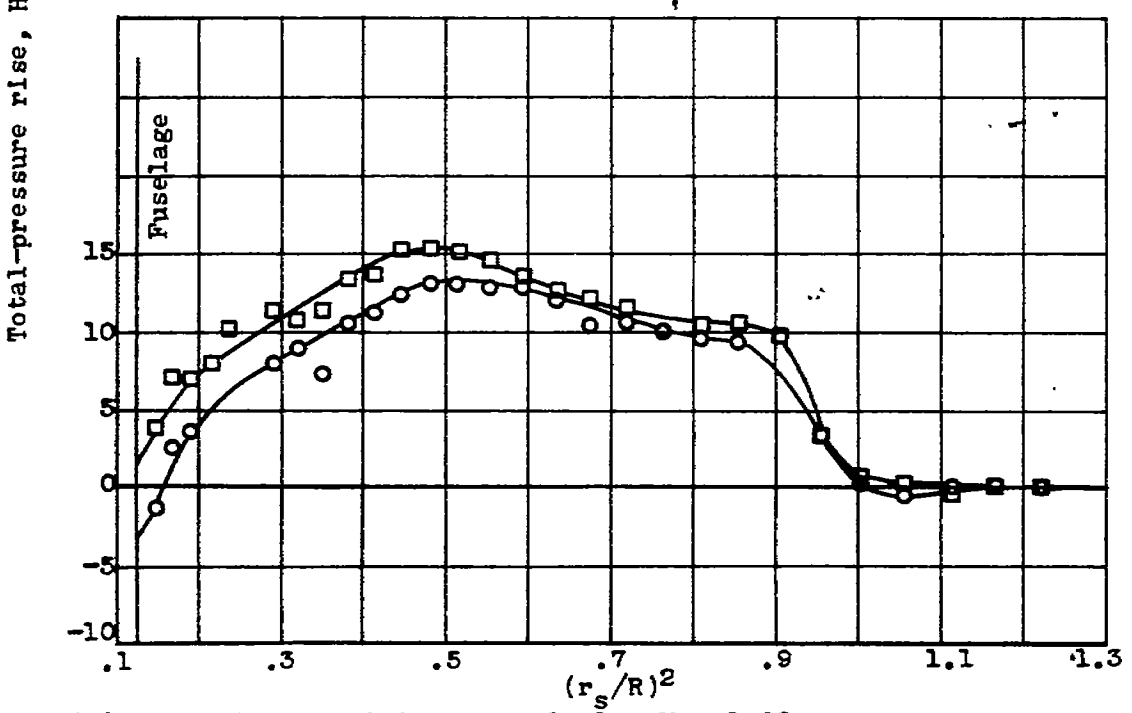

Total-pressure rise, $H_s - H_o$, lb/sq ft

(d) C_P, 0.20; J, 1.78; M_o, 0.51; M_t, 1.02.

Figure 18.- Concluded. Effect of advance-diameter ratio J on blade thruat load distribution at power coefficient C_P of approximately 0.20 and free-stream Mach number M_o of approximately 0.50. Curtiss 836-14C2-18R1 four-blade propeller.

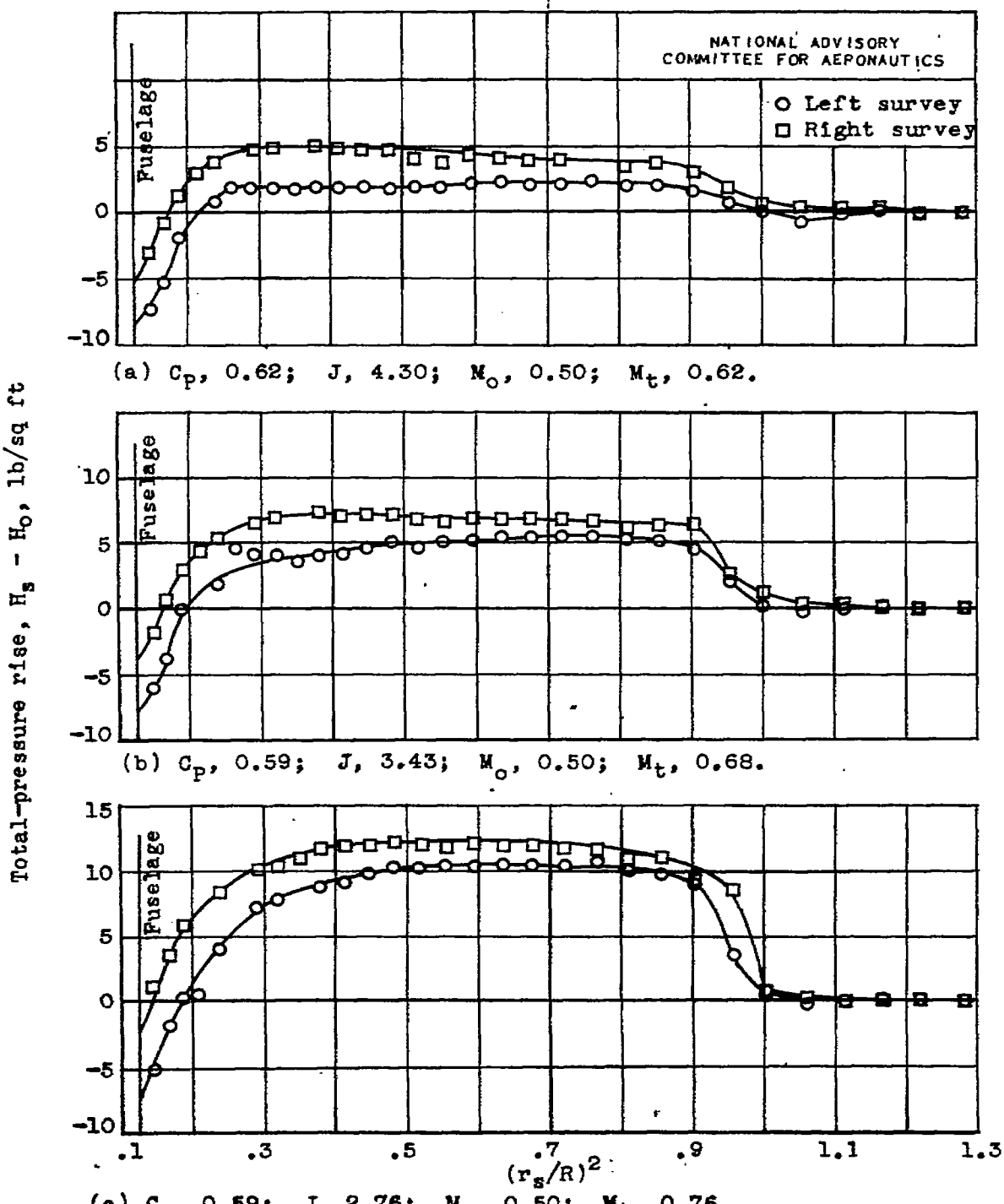

(a) C_p, 0.62; J, 4.30; M_o, 0.50; M_t, 0.62.

(b) C_p, 0.59; J, 3.43; M_o, 0.50; M_t, 0.68.

(c) C_p, 0.59; J, 2.76; M_o, 0.50; M_t, 0.76.

Figure 19.- Effect of advance-diameter ratio J on blade thrust load distribution at power coefficient C_p of approximately 0.60 and free-stream Mach number M_o of approximately 0.50. Curtiss 836-14C2-18R1 four-blade propeller.

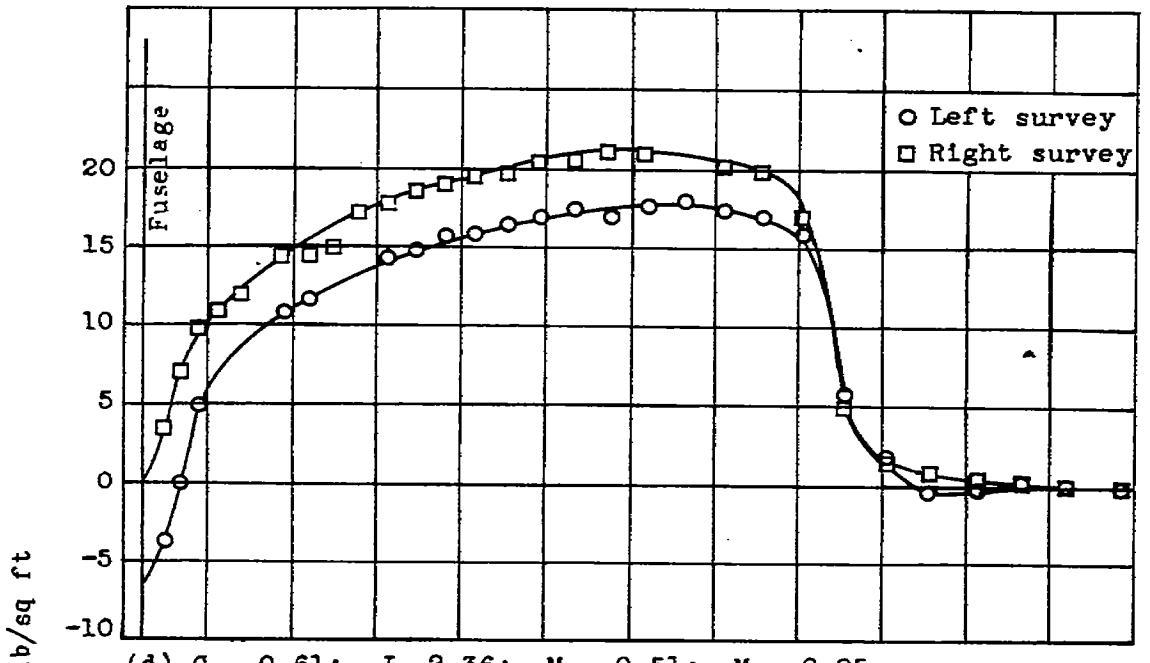

(d) C_p, 0.61; J, 2.36; M_o, 0.51; M_t, 0.85.

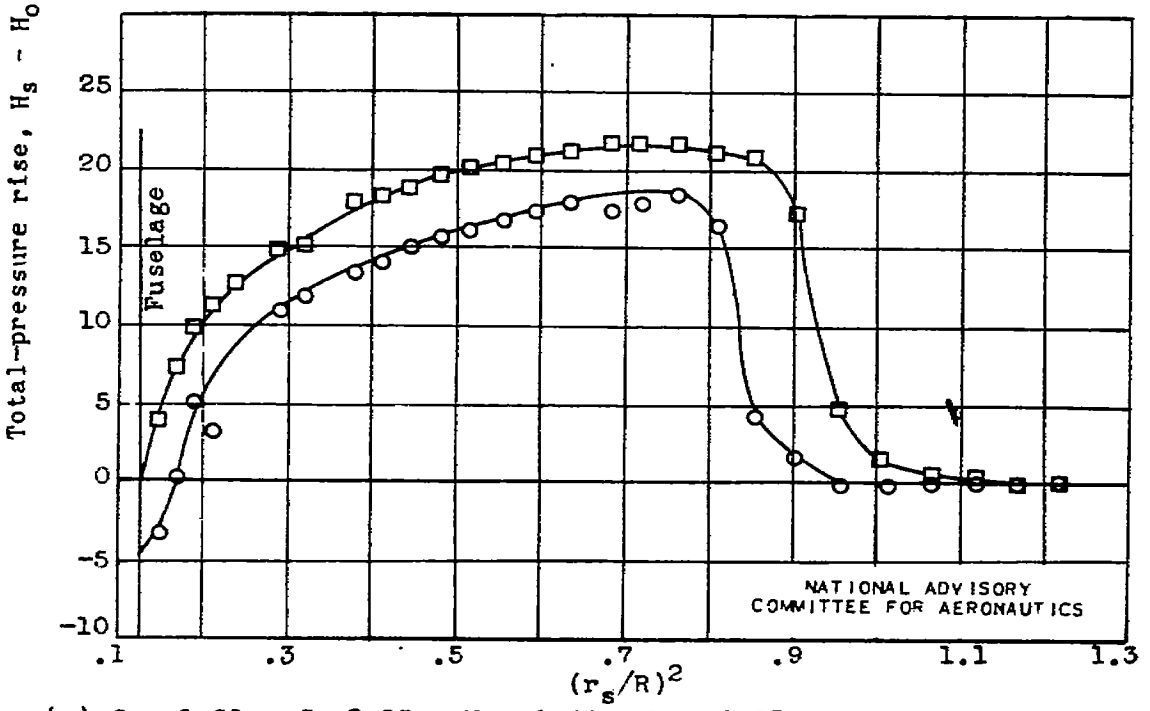

(e) C_p, 0.60; J, 2.25; M_o, 0.48; M_t, 0.83.

Figure 19.- Continued. Effect of advance-diameter ratio J on blade thrust load distribution at power coefficient C_p of approximately 0.60 and free-stream Mach number M_o of approximately 0.50. Curtiss 836-14C2-18R1 four-blade propeller.

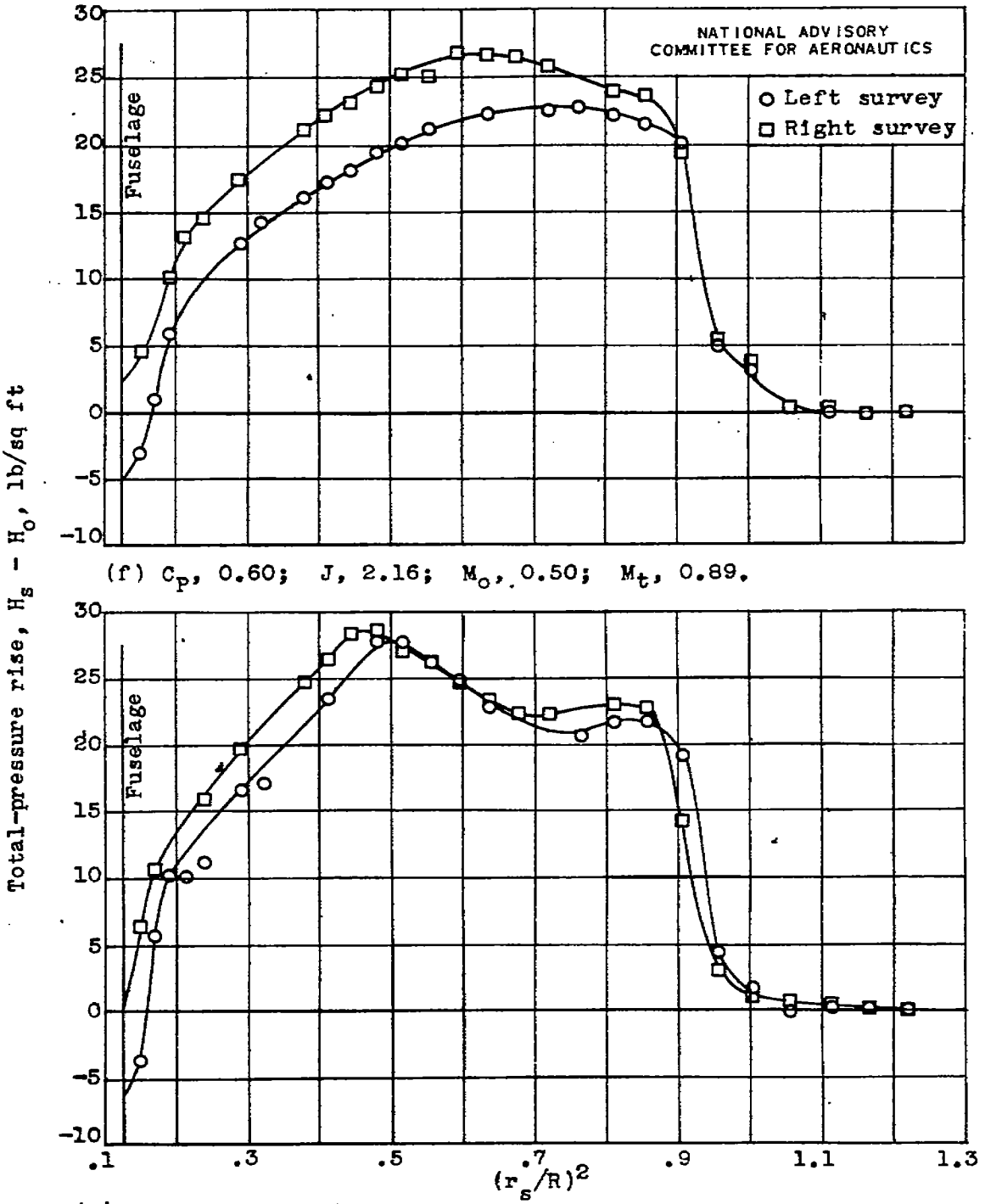

(f) C_p, 0.60; J, 2.16; M_o, 0.50; M_t, 0.89.

(g) C_p, 0.59; J, 1.70; M_o, 0.48; M_t, 1.01.

Figure 19.- Concluded. Effect of advance-diameter ratio J on blade thrust load distribution at power coefficient C_p of approximately 0.60 and free-stream Mach number M_o of approximately 0.50. Curtiss 836-14C2-18R1 four-blade propeller.

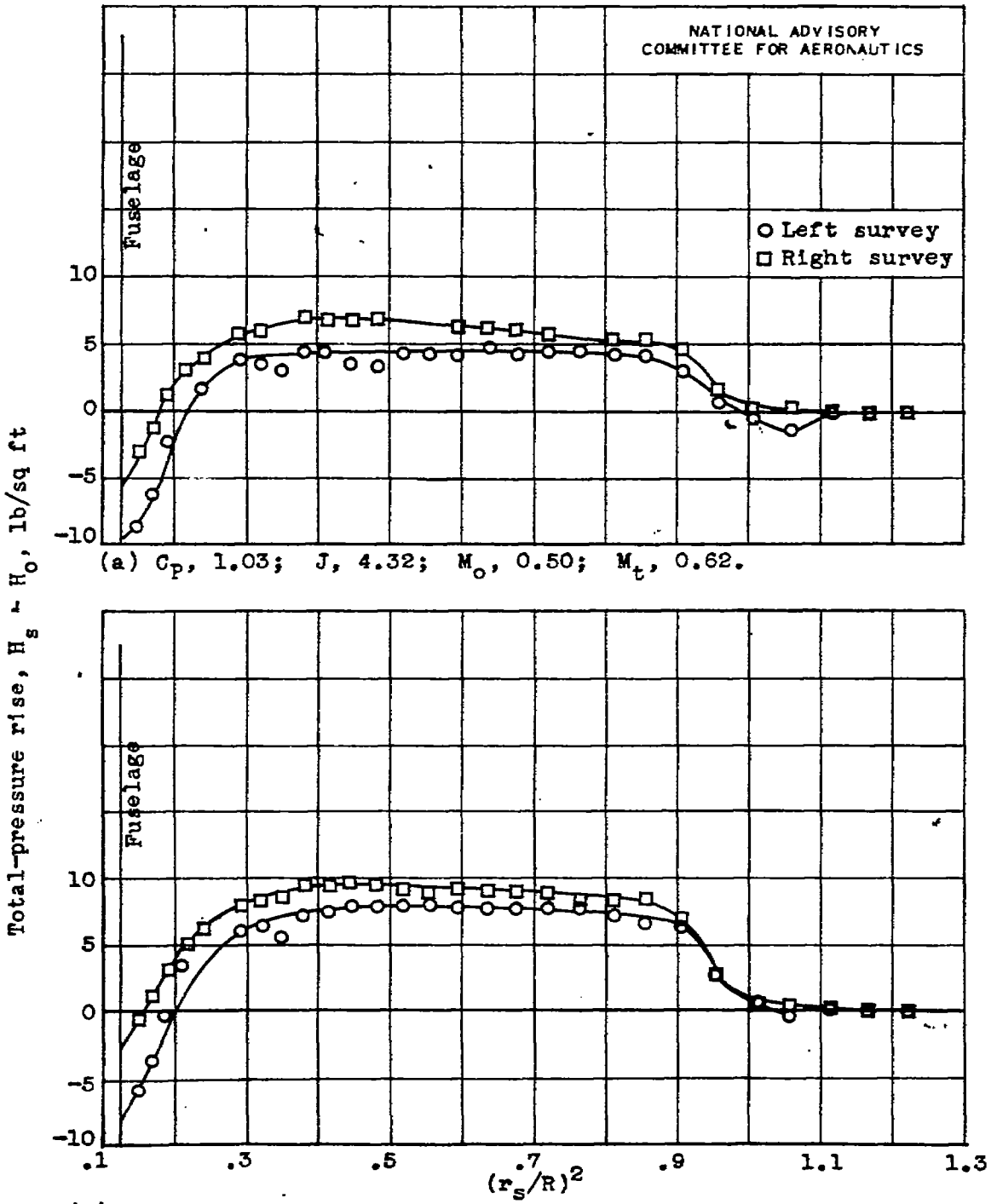

(a) C_p, 1.03; J, 4.32; M_o, 0.50; M_t, 0.62.

(b) C_p, 1.03; J, 3.68; M_o, 0.50; M_t, 0.66.

Figure 20.- Effect of advance-diameter ratio J on blade thrust load distribution at power coefficient C_p of approximately 1.00 and free-stream Mach number M_o of approximately 0.50. Curtiss 836-14C2-18R1 four-blade propeller.

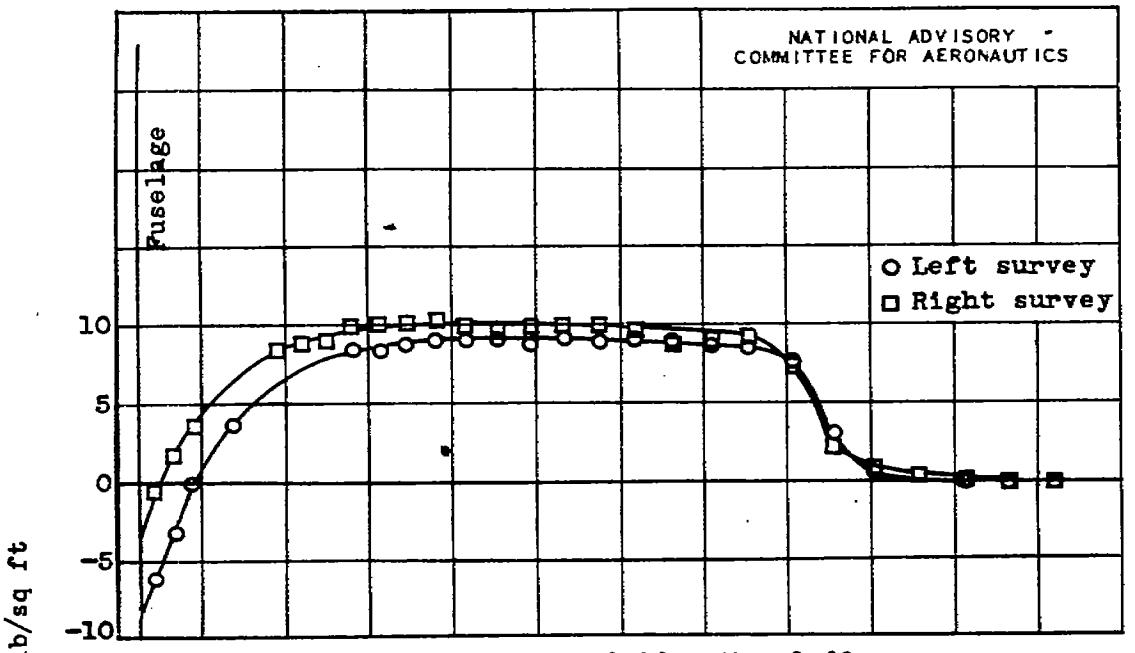

(c) C_p, 1.02; J, 3.42; M_o, 0.50; M_t, 0.68.

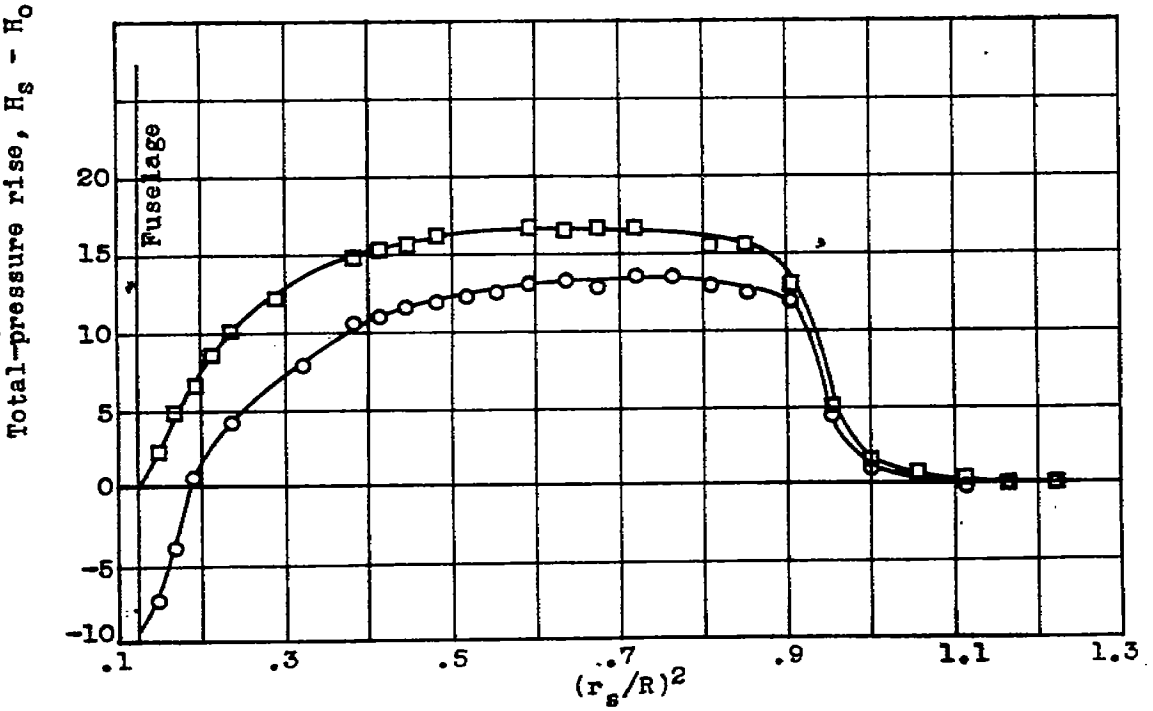

(d) C_p, 1.01; J, 3.04; M_o, 0.51; M_t, 0.73.

Figure 20.- Concluded. Effect of advance-diameter ratio J on blade thrust load distribution at power coefficient C_p of approximately 1.00 and free-stream Mach number M_o of approximately 0.50. Curtiss 836-14C2-18R1 four-blade propeller.